Simulating streamflow and dissolved organic matter export from a forested watershed

Na Xu,[1] James E. Saiers,[1] Henry F. Wilson,[1,2] and Peter A. Raymond[1]

Received 20 September 2011; revised 20 March 2012; accepted 26 March 2012; published 12 May 2012.

[1] Stream water concentrations of dissolved organic matter (DOM) exhibit large temporal variations during precipitation on forested, headwater catchments. We present a modeling framework appropriate for describing streamflow and event-driven export of DOM from small, forested watersheds. Our model links parametrically simple formulations for rainfall-runoff generation and soil water carbon dynamics. The rainfall-runoff formulation is developed by modifying the catchment model of Kirchner (2009) to account for hysteresis in the relationship between stream discharge and catchment water storage. Time series computations of catchment water storage are used by the soil carbon model to approximate the effects of leaching, adsorption, and mineralization on soil water DOM concentrations and the export of DOM from the terrestrial reservoir to the stream. Our findings show that this model is capable of reproducing hourly variations of stream discharge (ranging from 0.01 to 0.38 mm h^{-1}) and stream water DOM concentrations (ranging from 1.8 to 14 mg C L^{-1}) measured in a forested headwater stream in north central Massachusetts. Our analysis highlights the strong linkage between soil carbon dynamics and hydrological processes that govern catchment water storage and flow paths connecting the terrestrial system to the stream.

Citation: Xu, N., J. E. Saiers, H. F. Wilson, and P. A. Raymond (2012), Simulating streamflow and dissolved organic matter export from a forested watershed, *Water Resour. Res.*, *48*, W05519, doi:10.1029/2011WR011423.

1. Introduction

[2] Dissolved organic matter (DOM) that is present in stream waters plays an important role in aquatic ecosystem functioning and drinking water quality. DOM supplies nutrients and energy for heterotrophic bacteria in surface waters [*Duarte and Prairie*, 2005]. It forms complexes with metals and organic contaminants, thereby affecting their solubility, toxicity and transport properties [*Dunnivant et al.*, 1992; *Guggenberger et al.*, 1994]. DOM also influences stream water pH [*Bishop et al.*, 2000], affects light penetration [*Morris et al.*, 1995], and has implications to drinking-water treatment owing to formation of carcinogenic disinfection by-products through reactions with chlorine and bromine [*Chow et al.*, 2003].

[3] DOM concentrations in streams of forested, headwater catchments exhibit considerable temporal variability. Across base flow conditions, DOM concentrations vary over seasonal time scales with stream waters often (but not always) carrying higher concentrations of DOM during warm-weather months and shortly after leaf litter fall [*Hongve*, 1999; *Kohler et al.*, 2009]. Greater variations occur in response to rainfall and snowmelt events, when DOM concentrations may increase several fold relative to base flow levels [*Easthouse et al.*, 1992; *Buffam et al.*, 2001; *McClain et al.*, 2003]. This relationship between stream discharge and DOM concentrations implies that rainfall and snowmelt events may dominate watershed export of DOM. Although the role of hydrologic events in DOM export has not been quantified extensively, a recent analysis of stream discharge and DOM measurements from 30 forested watersheds in the eastern United States revealed that, on average, 86% of the DOM was exported during event flow conditions that constituted only 47% of the year [*Raymond and Saiers*, 2010].

[4] DOM in streams that drain forested, headwater catchments is primarily derived from the terrestrial landscape [*Schiff et al.*, 1990; *Brooks et al.*, 1999; *Palmer et al.*, 2001]. Consequently, stream water DOM concentrations depend, in part, on biogeochemical processes that govern varying rates of supply, mobilization, and retention of soluble organic matter within above- and below-ground reservoirs of the terrestrial environment [*Kalbitz et al.*, 2000; *Neff and Asner*, 2001; *Findlay and Sinsabaugh*, 2002]. These biogeochemical processes are, in turn, coupled with hydrological processes that govern the mixing of waters between surface and subsurface flow paths that connect the terrestrial system to the stream [*Hagedorn et al.*, 2000; *McGlynn and McDonnell*, 2003a; *Inamdar et al.*, 2006; *Inamdar and Mitchell*, 2007].

[5] The nonsteady nature of the hydrological and biogeochemical processes leads to considerable fluctuations in DOM concentrations between stream base flow and stormflow conditions in small, forested streams. Under base flow conditions, stream water DOM concentrations are typically low and comparatively stable [*Hope et al.*, 1994; *Mulholland and Hill*, 1997; *Buffam et al.*, 2001], which are characteristics commonly attributed to streamflow contributions

[1]School of Forestry and Environmental Studies, Yale University, New Haven, Connecticut, USA.
[2]Brandon Research Center, Agriculture and Agri-Food Canada, Brandon, Manitoba, Canada.

0043-1397/12/2011WR011423

from groundwater that has been depleted in organic matter because of sorptive interactions with the soil matrix and microbial mineralization [*Chorover and Amistadi*, 2001; *Michalzik et al.*, 2003]. With the onset of rainfall, downward infiltrating water and rising groundwater dissolve soluble soil organic matter and entrain microbial and root exudates present within shallow soil horizons [*Guggenberger et al.*, 1998; *Inamdar et al.*, 2004; *Pacific et al.*, 2009; *Austnes et al.*, 2010]. The DOM-laden water is transmitted rapidly toward the stream through permeable, near-surface flow pathways that may gain greater connectivity with increasing catchment wetness [*McGlynn and McDonnell*, 2003a]. The event-induced increases in stream water DOM concentrations are typically short-lived, with stream water DOM levels declining around the time of the peak in discharge hydrograph [*Laudon et al.*, 2004a; *Inamdar et al.*, 2006]. This pulse-like response suggests depletion of the organic matter pool as shallow surface horizons are flushed by percolating water [*Boyer et al.*, 1997], or alternatively, that subsurface reservoirs with low levels of DOM contribute proportionally more water to the stream over the later stages of the stormflow hydrograph [*Mulholland et al.*, 1990; *Hood et al.*, 2006]. If they are depleted by soil water flushing, terrestrial reserves of readily transportable DOM are replenished by biogeochemical processes at time scales on the order of hours to days, as punctuated increases in stream water DOM concentrations occur across successive rainfall events [*Hood et al.*, 2006].

[6] Current conceptualizations of coupled streamflow and DOM export processes have been formalized in mathematical models [*Grieve*, 1991; *Hornberger et al.*, 1994; *Boyer et al.*, 1996; *Canham et al.*, 2004; *Futter et al.*, 2007; *Yurova et al.*, 2008; *Jutras et al.*, 2011; *Schelker et al.*, 2011]. Few of these models, however, have been tested against data suitable for illuminating the dynamics of event-based DOM concentrations. A model proposed by *Hornberger et al.* [1994] and advanced by *Boyer et al.* [1996] linked TOPMODEL predictions of stream discharge with a chemical-mixing algorithm that approximated stream water DOM concentrations as the flow-weighted concentrations of DOM within shallow and deep subsurface reservoirs. Calculations of this model were found to be broadly consistent with weekly measurements of DOM concentrations made in a headwater stream near Montezuma, Colorado during spring snowmelt. More recently, *Futter et al.* [2007] developed a landscape-scale model of catchment carbon processing and surface water DOM fluxes (INCA). Evaluation of INCA against data collected from two Canadian headwater streams showed that the model is capable of simulating the intra-annual patterns of in-stream DOM concentrations, but that it underestimates stream water DOM concentrations during hydrologic events [*Futter et al.*, 2007].

[7] Published research lays the foundation for simulating stream water concentrations and fluxes of DOM, but predictive frameworks remain in their infancy and in need of improvement. The primary objective of our own work is to improve descriptions of the rapid changes in discharge and DOM concentrations that occur in forested, headwater streams during rainfall events. To accomplish this objective, we created a new model that links parametrically simple formulations for rainfall-runoff generation and soil water carbon dynamics. The rainfall-runoff formulation is developed by modifying the catchment model of *Kirchner* [2009] to account for hysteresis in the relationship between stream discharge and catchment water storage. Temporal changes in catchment water storage computed by the rainfall-runoff formulation are used by the soil water carbon formulation to simulate how biogeochemical processes change the stocks of terrestrial DOM that are flushed rapidly to the stream during stormflow events and exported more slowly from the catchment during base flow. Our findings show that this model is capable of reproducing high temporal resolution measurements of stream discharge and DOM concentrations made in a forested, headwater stream in north central Massachusetts over a 70 day calibration period that covered 8 stormflow events and over a monthlong validation period that covered five stormflow events.

2. Study Site and Data Collection

2.1. Site Description

[8] The study catchment is located in north central Massachusetts (42.5°N; 72°W) on the Prospect Hill tract of the Harvard Forest Long-Term Ecological Research (LTER) Site. This 24 ha headwater catchment is drained by the upper reaches of a stream called Bigelow Brook (Figure 1). Average annual temperature at the site is 8.5°C, and monthly mean temperatures range from −7°C in January to 19°C in July [*Currie et al.*, 1996]. Precipitation is distributed fairly evenly throughout the year and averages 1050 mm per year, with around 25% falling as snow [*Borken et al.*, 2006]. The snowpack covers the ground intermittently from late December to early April.

[9] Topography of the site is characterized by moderate relief, with land surface elevations ranging from 350 m at the watershed outlet to 400 m near the watershed divides. Ground surface slopes vary between 0% and 8% in the riparian zone and between 15% and 45% in the upland portions of catchment. The study site is under a mixed, primary growth stand with vegetation dominated by eastern hemlock (*Tsuga canadensis*). Other tree species within the upland and riparian zones include yellow birch (*Betula alleghaniensis*), American beech (*Fagus grandifolia*), striped maple (*Acer pensylvanicum*), and red maple (*Acer rubrum*) [*Collins et al.*, 2007].

[10] Soils here are generally rocky, well drained, and derived from glacial till deposits and metamorphic bedrock [*Currie et al.*, 1996]. They are mapped as Montauk series (coarse-loamy, mixed, mesic Typic Dystrochrepts) in the riparian zone and as Lyman series (loamy, isotic, frigid Lithic Haplorthods) in the upland by the USDA National Cooperative Soil Survey. Depth to bedrock averages on the order of 3 m and depends on the position along the hillslope. The soil profile contains well defined O and A horizons with a pH of approximately 3.5, and subsoil horizons with pH of 4.2–4.7 [*Currie et al.*, 1996; *Xu and Saiers*, 2010]. The organic matter content of the topsoil on the toe slope is reported to be 153 g C kg^{-1} [*Xu and Saiers*, 2010].

2.2. Meteorological and Hydrological Data

[11] Our study uses field meteorological and streamflow data that were collected as a part of the Harvard Forest LTER study. An automatic Fisher Meteorological Station, positioned 1.5 km from the Bigelow Brook watershed, measured air temperature, relative humidity, dew point, precipitation,

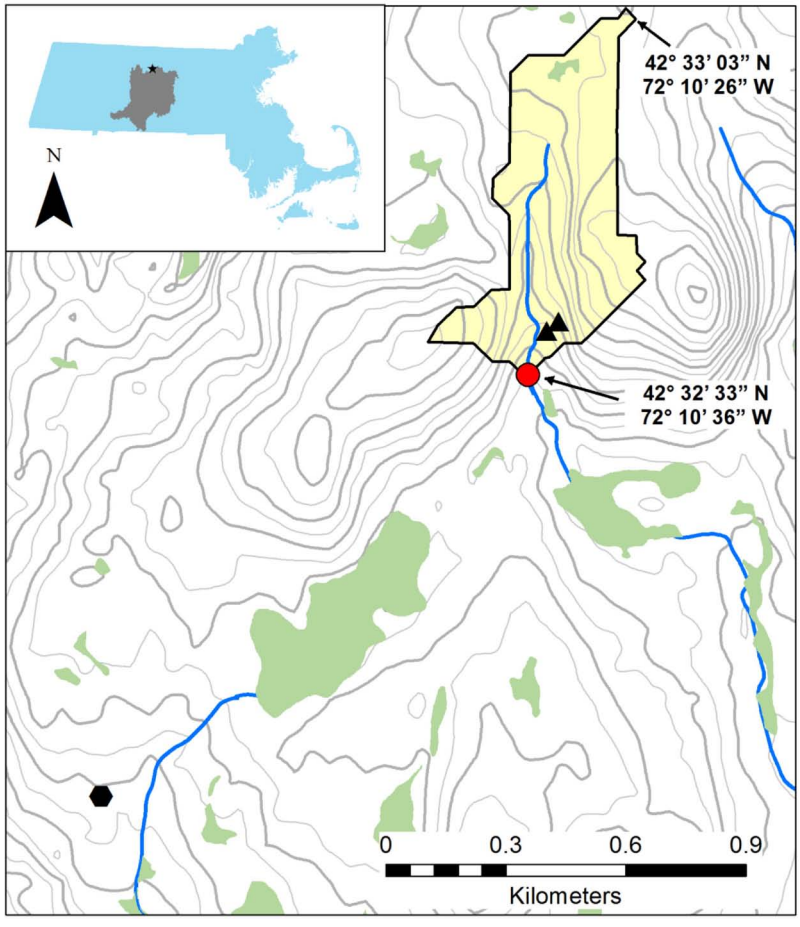

Figure 1. The Bigelow Brook study site within Harvard Forest in central Massachusetts. Instrumentation at the site includes a stream gauge (circle), groundwater wells (triangles), and a meteorological station (hexagon).

global solar radiation, photosynthetically active radiation, net radiation, barometric pressure, wind speed, and direction. These observations were made at 15 min intervals. Average daily soil temperatures at 10 cm depth were also recorded at the meteorological station and used in this study. Stream discharge at the watershed outlet was estimated at 15 min intervals from stream stage measurements collected with an automated water level recorder. For the analysis reported in this work, the 15 min meteorological and stream discharge data were aggregated to hourly sums. Two groundwater wells constructed of 5 cm (inner diameter) PVC pipe were installed within the watershed to measure water table elevation and to sample groundwater for chemical analysis. One well was positioned at the toe slope approximately 13 m from the stream, and the other well was positioned in the upland approximately 26 m from the stream (Figure 1). The toe slope well was installed to a depth of 3 m and bottomed within the soil profile, while the upslope well was installed to a depth of 5.4 m and penetrated roughly 3 m into bedrock. Pressure transducers (Campbell® Scientific) were placed in the wells and connected to an electronic data logger in order to continuously monitor water table levels.

2.3. Stream Water DOM Data

[12] High temporal resolution estimates of stream water DOM concentrations appropriate for resolving event-based variability in DOM fluxes were obtained from measurements of fluorescent dissolved organic matter (FDOM). Published research indicates that a linear relationship exists between FDOM measurements and DOM concentrations in filtered or low-turbidity water samples [*Saraceno et al.*, 2009]. In this study, the FDOM readings were collected using a Turner Designs Cyclops-7 colored dissolved organic matter (CDOM) fluorometer probe connected to a Campbell CR-1000 data logger. The CDOM probe uses an LED light source to excite DOM molecules with the peak intensity at 370 nm and measures the intensity of fluorescence emission with a peak transmissivity at 470 nm. The probe was placed near the stream discharge station in a shaded location facing the direction of stream water flow and cleaned monthly to avoid biofouling.

[13] A calibration curve was constructed to convert the FDOM measurements to stream water DOM concentrations. The DOM concentrations used for the calibration curve were determined on water samples collected at high frequency during select rainfall events and at longer intervals under base flow conditions. All water samples were kept on ice until filtration, and filtered through a rinsed Millipore polycarbonate filter (0.22 micron pore size) within 36 h of the time of sampling. DOM concentrations were analyzed by combustion with a Shimadzu TOC-VCSH analyzer. The calibration curve created by plotting

DOM concentrations in the stream water samples against FDOM measurements recorded in the field at corresponding times was linear ($R^2 = 0.95$; $p < 0.001$) for DOM concentrations ranging from 0.5 mg C L^{-1} to 22 mg C L^{-1}.

3. Model Formulation

3.1. Rainfall-Runoff Model

[14] *Kirchner* [2009] derived a single equation rainfall-runoff model that links rainfall and evapotranspiration to streamflow. This model, which we refer to as the Kirchner model, is parsimonious in its structure and parameterization yet describes stream discharge with equal or better success than more highly parameterized models [*Bathurst*, 1986; *Polarski*, 1997]. In developing the model, *Kirchner* [2009] assumed that discharge could be interpreted as a single-valued function of catchment water storage. Our initial analysis revealed that this assumption is not fully appropriate for describing streamflow fluctuations within the Bigelow Brook Watershed; therefore, we modified the approach of *Kirchner* [2009] to account for hysteresis in the discharge-storage relationship.

[15] The Kirchner model, like most physically based models of catchment hydrology, is governed by the equation for the conservation of water mass:

$$\frac{dS}{dt} = P - ET - Q \tag{1}$$

where S is the total water storage in the catchment (mm), P is the precipitation (mm h^{-1}), ET is actual evapotranspiration (mm h^{-1}), and Q is the stream discharge (mm h^{-1}). The four variables S, P, ET, and Q are functions of time and considered to be averaged over the whole catchment. It should be noted that S refers to the water stored within the portion of the catchment that contributes to streamflow generation and thus includes waters in both the saturated and unsaturated zones.

[16] *Kirchner* [2009] assumed that Q depends solely on S, such that

$$Q = f(S). \tag{2}$$

This assumption is a valid approximation in many small catchments [*Laudon et al.*, 2004b; *Kirchner*, 2009; *Majone et al.*, 2010], but may be invalid if, for example, direct precipitation onto the stream or saturated excess overland flow ("bypassing flow") is a dominant component of discharge [*Kirchner*, 2009]. The assumption expressed by (2) also implies that hydraulic connectivity exists between the dynamical saturated and unsaturated storage zones of the catchment [*Teuling et al.*, 2010].

[17] If the storage-discharge relationship can be represented as a single-valued function, equation (2) is invertible (i.e., $S = f^{-1}(Q)$) and thus dQ/dS can be expressed as a function of Q:

$$\frac{dQ}{dS} = f'(S) = f'\left(f^{-1}(Q)\right) = g(Q). \tag{3}$$

where $g(Q)$ quantifies the sensitivity of discharge to changes in catchment storage and hence is referred to as the catchment sensitivity function (Figure 2). Differentiating equation (2) with respect to time and substituting equations (1) and (3) into the result leads to a first-order differential equation for describing the rate of change of discharge (Q) with time:

$$\frac{dQ}{dt} = \frac{dQ}{dS}(P - ET - Q) = g(Q) \cdot (P - ET - Q). \tag{4}$$

Equation (4) is the key governing equation of the Kirchner Model. Its integration yields the stream discharge hydrograph as influenced by temporal variations in precipitation and evapotranspiration and the watershed's characteristic sensitivity function, dQ/dS.

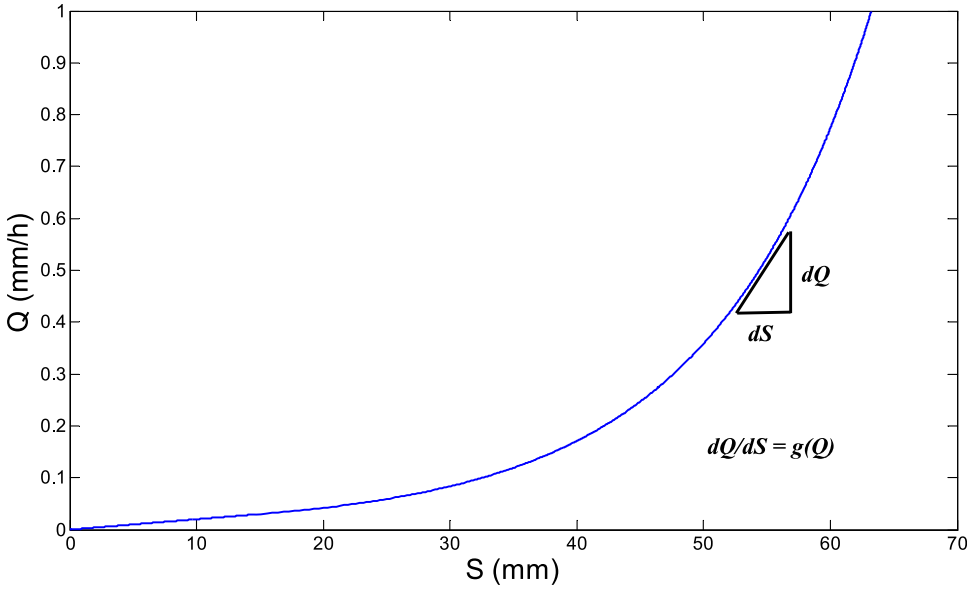

Figure 2. Single-valued discharge-storage relationship of the type used by *Kirchner* [2009] for stream-discharge simulation. The slope of the curve, $dQ/dS = g(Q)$, is referred to as the discharge sensitivity.

[18] The sensitivity function depends, in some unknown way, on watershed properties and must be inferred from streamflow data through analysis of recession plots or time series measurements of stream discharge. *Kirchner* [2009] showed, for example, an expression for $g(Q)$ as a quadratic in logs is appropriate for quantifying discharge time series for two streams that drain headwater catchments in Wales. *Teuling et al.* [2010] tested the approach by *Kirchner* [2009] using a piecewise linear sensitivity function in double-log space and succeeded in simulating streamflow dynamics in the Swiss Rietholzbach catchment.

[19] In this work, we introduce a way to represent hysteresis in the Q-S relationship that defines the sensitivity function. A hysteretic Q-S relationship exhibits path dependence such that stream discharge depends on the history of catchment storage, in addition to the value of storage itself. Thus, a single Q-S curve that is characteristic of the catchment does not exist, but instead a potentially infinite number of curves exist that depend on whether the catchment is gaining or losing water and on the past pattern of catchment wetting and drying. Observations of Q-S hysteresis have been widely reported [*Kendall et al.*, 1999; *Ewen and Birkinshaw*, 2007; *Hrncir et al.*, 2010], although the mechanisms responsible for this hysteretic behavior are difficult to ascertain with certainty.

> *Beven* [2006, p. 611] suggests that hysteresis in the storage-discharge relationship is attributable to a number of factors including hysteresis in the small-scale matrix soil characteristics, the possibility of changing vertical and downslope connectivities of flow pathways as the soils dries and rewets, the possibility of by-passing of available matrix storage by preferential flows and fingering during wetting, the possibility of threshold effects in local flux storage relationships, the development of inter-unit patterns of antecedent wetness, dynamics of contributing areas, spatial structure in soil depths and permeabilities that might lead to perched saturation or other complex flow pathways and the effects of routing delays within the unit.

[20] Hysteretic phenomena are observed in a many fields of science and engineering and hence have been represented mathematically in numerous fashions [*Bertotti and Mayergoyz*, 2006; *Beven*, 2006; *Ikhouane and Rodellar*, 2007]. Within the earth sciences, considerable attention has been devoted to accounting for hysteresis in the moisture characteristic curves of soils, or, in other words, the relationship between capillary pressure (Ψ) and volumetric moisture (Θ). *Parker and Lenhard* [1987], for example, presented a widely used approach for Ψ-Θ hysteresis that involves interpolation and scaling of measurements of a soil's primary imbibition and drainage curves. By generalizing the approach of *Parker and Lenhard* [1987], we were unable to account for Q-S hysteresis appropriately within the context of Kirchner Model. Instead, we adopted an alternative approach that describes Q-S hysteresis as a piecewise linear function.

[21] We approximate the Q-S relationship with three piecewise linear segments that correspond to three different stages of catchment wetting and drying (Figure 3). These stages are (1) imbibition, when the catchment gains water in response to rainfall; (2) fast-recession drainage, the period of declining discharge and catchment water storage occurring immediately after the peak in the stormflow hydrograph; and (3) base flow recession drainage, which corresponds to periods of catchment water loss associated with stream base flow conditions. Given that the three segments of the Q-S relationship are linear, the sensitivity function (i.e., slope) for each segment is constant, such that

$$g(Q) = m_i\,, \qquad \frac{dQ}{dt} \geq 0 \tag{5a}$$

$$g(Q) = m_{fd}\,, \qquad \frac{dQ}{dt} < 0,\ Q \geq Q_{anc} \tag{5b}$$

$$g(Q) = m_{bd}, \qquad \frac{dQ}{dt} < 0,\ Q < Q_{anc} \tag{5c}$$

where m_i, m_{fd}, and m_{bd} are the slopes of the Q-S relationship corresponding to catchment imbibition, fast-recession

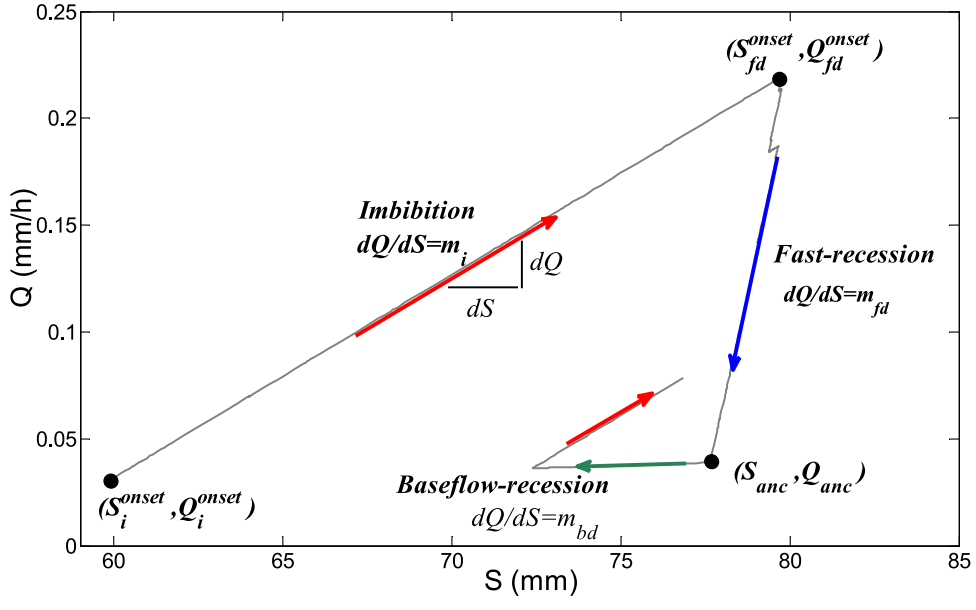

Figure 3. Schematic diagram of discharge sensitivity (dQ/dS) and the hysteretic Q-S characteristic curve for watershed wetting and drying.

drainage, and base flow recession drainage, respectively (Figure 3). The variable Q_{anc} is the value of stream discharge that separates the fast-recession and base flow recession periods (Figure 3); it is not a constant, but depends on the slopes of the piecewise linear segments and notably on the history of modeled discharges:

$$Q_{anc} = \frac{Q_{fd}^{onset} - m_{fd}\left[\frac{Q_{fd}^{onset} - Q_i^{onset}}{m_i} + \frac{Q_i^{onset}}{m_{bd}}\right]}{m_{bd} - m_{fd}} \times m_{bd} \tag{6}$$

where Q_i^{onset} and Q_{fd}^{onset} are model-computed discharges at the onset of the most recent periods of catchment imbibition and fast-recession drainage, respectively (Figure 3).

[22] The model computations of catchment water storage (S) depend on the past trajectory and magnitude of Q and can be expressed in terms of the segment slopes of the piecewise linear distribution function:

$$S - S_0 = \frac{(Q - Q_i^{onset})}{m_i} + \frac{Q_i^{onset}}{m_{bd}}, \qquad \frac{dQ}{dt} \geq 0 \tag{7a}$$

$$S - S_0 = \frac{(Q - Q_{fd}^{onset})}{m_{fd}} + \frac{Q_i^{onset}}{m_{bd}} + \frac{Q_{fd}^{onset} - Q_i^{onset}}{m_i}, \quad \frac{dQ}{dt} < 0, \quad Q \geq Q_{anc} \tag{7b}$$

$$S - S_0 = Q/m_{bd}, \qquad \frac{dQ}{dt} < 0, \quad Q < Q_{anc} \tag{7c}$$

where S_0 is a reference storage level. Assignment of S_0 is generally arbitrary because the system's bottom boundary is rarely known in the field. We assign a value of zero to S_0 for the simplicity of calculation in the present study.

[23] Equations (4)–(7) then describe the temporal variability in streamflow for the case in which the stream discharge can be approximated as a piecewise linear function of catchment water storage. We solved these equations numerically using a variable-order routine (ODE15s) within MATLAB subject to the constraint that the initial value of Q corresponded with a period of base flow recession. Running calculations of catchment inflows, outflows, and storage showed that errors in the water mass balance did not exceed 2% for any of the simulations reported in this study.

[24] Numerical solution of the governing equations for two hypothetical rainfall events illustrates the linkage between the piecewise linear Q-S function and the model-computed hydrograph (Figure 4). During periods of catchment imbibition (i.e., periods 1 and 4), the Q-S relationship is determined, in part, by its constant slope (m_i) and also by stream discharge at the onset of imbibition (Q_i^{onset}), which, in turn, is influenced by history of wetting and drying within the catchment. The relationship between Q and S during periods of fast recession (i.e., periods 2 and 5) is similarly nonunique, reflecting the past trajectory of discharge. During base flow recession (periods 3 and 6), the Q-S relationship is single valued and independent of historical changes in streamflow. Owing to its hysteretic nature, the Q-S relationship cannot be specified a priori, but rather

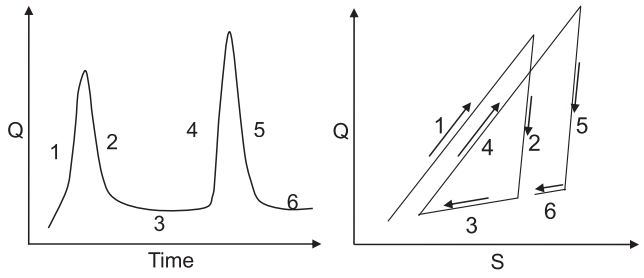

Figure 4. Explanatory diagram for the Q-S hysteretic relationship: (left) example hydrograph and (right) the corresponding time-evolving Q-S relationship.

its appearance, though constrained by the slopes of its linear segments, is determined by past patterns of rainfall, evapotranspiration, and streamflow.

3.2. Dissolved Organic Matter Mixing and Reaction Model

[25] The purpose of the DOM model is to simulate temporal changes in stream water DOM concentrations that result from the export of carbon from the terrestrial landscape. A mass balance on DOM within the waters of the terrestrial reservoir forms the basis of the model. We make the simplifying assumption that the terrestrial reservoir is well mixed with respect to DOM and hence DOM concentrations in stream water (C_{str}) equal DOM concentrations in the terrestrial reservoir (C_{Tres}). The DOM model is coupled to the rainfall-runoff model (see section 3.1) through catchment water storage (S), as the product of C_{Tres} and S yields the mass of DOM within the terrestrial reservoir.

[26] The rate of change of DOM mass within the terrestrial reservoir reflects changes in catchment water storage and associated biogeochemical processes, including dissolution and desorption reactions that generate DOM from solid organic matter, adsorption and degradation of soil water DOM, and flushing of DOM by rain water that is routed through the catchment to stream. In its most general form, the DOM mass balance equation can be expressed as

$$\left.\frac{d(S \cdot C_{Tres})}{dt}\right|_{total} = \left.\frac{d(S \cdot C_{Tres})}{dt}\right|_{fstrel} + \left.\frac{d(S \cdot C_{Tres})}{dt}\right|_{slwrel} + \left.\frac{d(S \cdot C_{Tres})}{dt}\right|_{ads\&deg} + \left.\frac{d(S \cdot C_{Tres})}{dt}\right|_{flush}. \tag{8}$$

Equation (8) approximates $\left.\frac{d(S \cdot C_{Tres})}{dt}\right|_{total}$, the temporal change in the total mass of DOM within the terrestrial reservoir, as the sum of changes due to biogeochemical reactions that govern the fast release (*fstrel*) and slow release (*slwrel*) of DOM into the soil water, adsorption and degradation reactions (*ads&deg*) that remove DOM from the soil water, and soil water flushing (*flush*).

[27] We assume that DOM is released rapidly into the soil water during precipitation events as infiltrating water and a rising water table leach readily soluble organic matter composed of leaf litter and freshly formed soil organic matter that lies near the land surface. Laboratory studies demonstrate that DOM concentration leached from Harvard

Forest topsoil can be as high as 110 mg C L^{-1} at the onset of a rainfall event, and the supply of readily leachable DOM is not depleted throughout the course of 610 mm rainfall [*Xu and Saiers*, 2010]. This release of DOM is precipitation driven and occurs in an ephemeral fashion when stream discharge, and hence catchment storage, are elevated above conditions that typify base flow. We treat DOM generation from the readily soluble fraction of solid organic matter as a linear, instantaneous (equilibrium) reaction describable by

$$C_{Tres} = O_{rs}/k_p \tag{9}$$

which leads to

$$\left.\frac{d(S \cdot C_{Tres})}{dt}\right|_{fstrel} = \frac{1}{k_p}\frac{d(S \cdot O_{rs})}{dt}, \qquad Q \geq Q_{anc} \tag{10}$$

where O_{rs} (mg C kg^{-1}) is the concentration of readily soluble organic matter and k_p (L kg^{-1}) is an equilibrium partition coefficient. If temporal changes in O_{rs} are small, which may be the case for the relatively short (monthly) time scales tested in this study [*Boone*, 1994], then $dO_{rs}/dt \approx 0$ and equation (10) reduces to

$$\left.\frac{d(S \cdot C_{Tres})}{dt}\right|_{fstrel} = \frac{1}{k'_p}\frac{dS}{dt}, \qquad Q \geq Q_{anc} \tag{11}$$

where $k'_p = k_p/O_{rs}$. Consistent with our assumption that fast generation of DOM is associated with periods of precipitation, equation (11) applies only under stormflow conditions, when $Q \geq Q_{anc}$. Under base flow conditions, when stream discharge and catchment water storage are low, near-surface horizons that are rich in soluble organic matter are disconnected from the stream and insufficiently wet to support the rapid production of significant quantities soil water DOM and thus

$$\left.\frac{d(S \cdot C_{Tres})}{dt}\right|_{fstrel} = 0, \qquad Q < Q_{anc}. \tag{12}$$

[28] The fast release of soil water DOM is accompanied by a second modeled reaction that represents the influences of mechanisms that govern slow, rate-limited generation of soil water DOM. This generation may arise from dissolution reactions involving relatively old and more complex soil organic matter, desorption of DOM from mineral-rich soil horizons, and, perhaps, microbial and root exudation [*Kaiser and Zech*, 1999; *Munch et al.*, 2002; *Yano et al.*, 2004]. We lump these mechanisms and approximate their contributions to the slow release of DOM by

$$\left.\frac{d(S \cdot C_{Tres})}{dt}\right|_{slwrel} = k_{sr}S \tag{13}$$

where k_{sr} (mg C L^{-1} h^{-1}) is a coefficient that quantifies rate-limited (slow) release of DOM into the soil water. Equation (13) implies that, in the absence of changes in storage (i.e., $dS/dt = 0$), the rate of change in soil water DOM concentrations due to this lumped, kinetics reaction is constant.

[29] DOM that is mobilized within the water of the terrestrial reservoir does not travel conservatively, but is susceptible to removal through adsorption and through degradation reactions involving the soil microbial community. We describe these processes as first-order kinetics reactions, such that

$$\left.\frac{d(S \cdot C_{Tres})}{dt}\right|_{ads\&deg} = -k_{ads}C_{Tres}S - k_{\deg}C_{Tres}S = -k_{rem}C_{Tres}S \tag{14}$$

where k_{ads} (h^{-1}) and k_{deg} (h^{-1}) are rate coefficients for the adsorption and degradation of soil water DOM, respectively, and k_{rem} (h^{-1}), the rate coefficient for total soil water DOM removal, equals the sum of k_{ads} and k_{deg}.

[30] The final term of equation (8) accounts for the influence of hydrological processes on the carbon balance. It describes changes in the terrestrial stores of organic carbon that occur as soil water DOM is transported along subsurface pathways to the stream. Given our approximation that the terrestrial reservoir is well mixed with respect to DOM concentrations, the time rate of change in DOM mass due to flushing of this reservoir is

$$\left.\frac{d(S \cdot C_{Tres})}{dt}\right|_{flush} = -QC_{Tres} \tag{15}$$

where Q, the stream discharge, is computed as a function of time by the rainfall-runoff model.

[31] Substitution of equations (11) – (15) into equation (8) yields the complete form of the conservation of mass statement that governs the DOM model:

$$\left.\frac{d(S \cdot C_{Tres})}{dt}\right|_{total} = \frac{1}{k'_p}\frac{dS}{dt} + k_{sr}S - k_{rem}C_{Tres}S - QC_{Tres}. \tag{16}$$

By rearranging (16) and by recognizing that resident and outflow DOM concentrations from the well-mixed terrestrial reservoir are identical, the mass balance expression for the DOM model can be expressed in terms of the temporal derivative of stream water DOM concentrations (C_{str}):

$$\frac{dC_{str}}{dt} = \frac{dC_{Tres}}{dt} = \left(k_{sr}S - k_{rem}C_{Tres}S - QC_{Tres} + \left[\frac{1}{k'_p} - C_{Tres}\right]\frac{dS}{dt}\right)/S \tag{17}$$

Equation (17) includes three parameters that describe production and consumption of soil water DOM: k'_p, k_{sr}, and k_{rem}. Values of these parameters quantify effective averages of equilibrium partitioning and reaction rates that vary spatially throughout the watershed owing to heterogeneity in watershed properties, such as soil texture, soil moisture, and the composition of soil organic matter and soil water DOM. The characteristics of DOM production and consumption also exhibit temporal variation owing to the sensitivity of these processes to changes in time-varying properties, such as temperature and soil moisture. While the

model coefficients could be expressed as functions of soil temperature and catchment water storage (as a surrogate for average soil moisture) as described, for example, by *Hornberger et al.* [1994], *Futter et al.* [2007], and *Yurova et al.* [2008], we tested a more parsimonious approach by treating these coefficients as constants. This simplification is likely inappropriate for simulation of watershed DOM export for periods that extend over seasons, but may be suitable for resolving subdaily changes in stream water DOM concentrations over intraseasonal time scales.

3.3. Model Calibration, Testing, and Goodness-of-Fit Metrics

[32] Model execution requires time series estimates of rainfall and actual evapotranspiration, as well as specification of the model parameters that govern streamflow generation and production and consumption of DOM. Fifteen minute interval rainfall data recorded at the rain gauge located 1.5 km from Bigelow Brook (see section 2.2) were used as catchment-averaged estimates of rainfall. Catchment-averaged evapotranspiration (ET) was approximated at the same temporal resolution by rescaling calculations of potential evapotranspiration (ET_0) by an adjustable coefficient, k_E, such that $ET = ET_0{}^* k_E$. To compute ET_0, the meteorological measurements described in section 2.2 were used in the Penman-Monteith equation [*Allen et al.*, 1998]. The ratio of ET to ET_0 is sensitive to changes in soil wetness; therefore, our specification of a single-valued k_E reflects the assumption that frequent rainfall during the study period maintained the wetness of near-surface soils at levels sufficient to moderate changes in evaporative stress.

[33] The parameters of the discharge sensitivity function (i.e., m_i, m_{fd}, and m_{bd}) were estimated together with k_E by calibrating the model to stream discharge data collected during October and November in 2010. Parameters for production and consumption of DOM (i.e., k'_p, k_{sr}, and k_{rem}) were estimated by calibrating the model to data on stream water DOM concentrations measured over the same 2 month period. In these inversions, a Levenberg-Marquadt algorithm was used to find the values of parameters that minimized the sum-of-squared-errors objective functions for stream discharge and DOM concentrations. The calibrated model was tested against data recorded outside the period of calibration. This test involved using the parameters estimated from calibration (without further adjustment) to simulate stream discharge and DOM concentrations during October 2009. During both the calibration and verification periods, the catchment gained water in response to multiple rainfall events and thus comparison of measurements and model calculations during these times enabled evaluation of the ability of the model to reproduce storm event fluxes of DOC that dominate the annual DOC export form the watershed.

[34] For both the inverse and forward simulations, the overall goodness-of-model fit was assessed through calculation of the Nash-Sutcliffe efficiency (R^2) [*Nash and Sutcliffe*, 1970],

$$R^2 = 1 - \frac{\sum (o_i - m_i)^2}{\sum (o_i - \overline{o})^2} \tag{18}$$

where o_i and m_i are the observed and modeled time series values, respectively, and $\overline{o}$ is the mean of the observed values. Separate values of the R^2 were computed for the simulations of stream discharge and stream water DOM concentrations. We also quantified the agreement between peak values of stream discharge and DOM concentration measured during storm events and corresponding model-simulated values. The goodness-of-peak fit was computed as [*Green and Stephenson*, 1986]

$$GOP = 1 - \frac{1}{n}\sum_{i=1}^{n} \frac{|P_{oi} - P_{mi}|}{P_{oi}} \tag{19}$$

where P_{oi} and P_{mi} are the observed and modeled peak values of stream discharge or DOM concentration associated with the ith storm event, respectively, and n is the total number of storm events. The goodness-of-peak fit increases with the value of GOP, such that a GOP value of unity corresponds to an exact match between measured and modeled peak values. A third model fitness metric compares measured and modeled values for the volume of water (GOM_W) and mass of DOM (GOM_C) exported during storm events. This metric is computed on the basis of the areas beneath the storm event portions of the discharge hydrograph and DOM chemograph, such that

$$GOM_W = 1 - \frac{1}{n}\sum_{i=1}^{n} \left(\frac{\left| \int_{B_i}^{E_i} Q_o dt - \int_{B_i}^{E_i} Q_m dt \right|}{\int_{B_i}^{E_i} Q_o dt} \right)_i \tag{20a}$$

$$GOM_C = 1 - \frac{1}{n}\sum_{i=1}^{n} \left(\frac{\left| \int_{B_i}^{E_i} Q_o C_o dt - \int_{B_i}^{E_i} Q_m C_m dt \right|}{\int_{B_i}^{E_i} Q_o C_o dt} \right)_i \tag{20b}$$

where Q is discharge (mm h^{-1}); C is stream water concentration of DOM (mg C L^{-1}); the subscripts o and m refer to observed and modeled values, respectively, B_i is the time corresponding to the beginning of the ith storm event, E_i is the time corresponding to the end of the ith storm event, and n is the number of storm events. The integral terms in (20a) represent the cumulative volume of water exported during storm event i, while the integral terms in (20b) represent the cumulative mass of DOM exported in storm event i. GOM equals unity when the model describes observations of storm event water and DOM export exactly.

4. Results

4.1. Field Observations of Fall 2010

4.1.1. Rainfall-Runoff Characteristics

[35] We calibrated the model against data collected over a 2 month period spanning from October to November 2010 (Figure 5a). During this time, stream discharge varied between 0.01 and 0.38 mm h^{-1}, and eight stormflow events could be discerned from the stream hydrograph. The rainfall-runoff ratio was 0.23 for the entire period and ranged from 0.1–0.4 on a storm event basis. Streamflow was generally flashy, responding quickly to precipitation and declining to base flow conditions within two days after rainfall ceased. Although stream

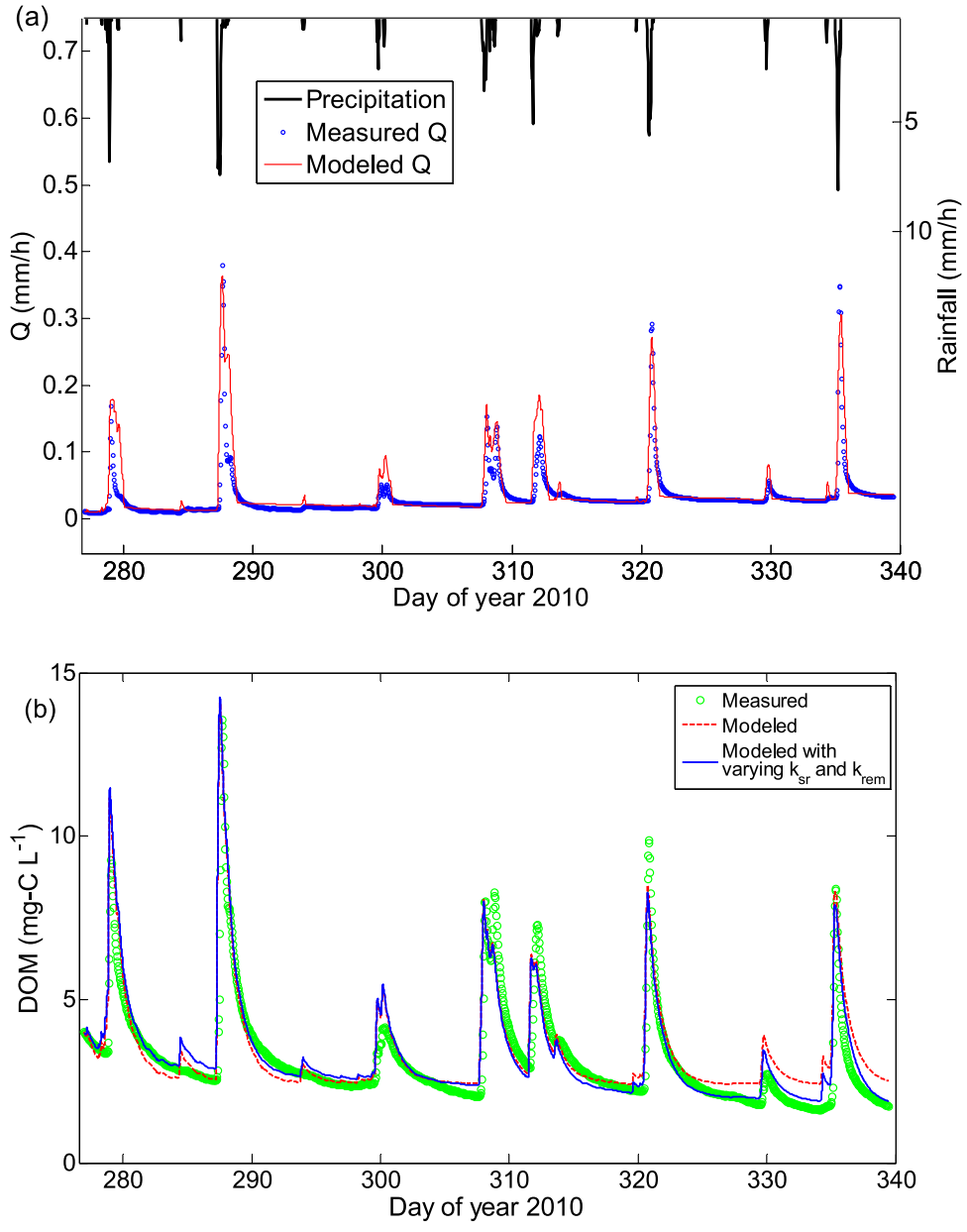

Figure 5. Field observations and model simulations for fall 2010: (a) measurements of precipitation and stream discharge and calculations of stream discharge made with a version of the rainfall-runoff model that accounts for *Q*-*S* hysteresis and (b) measured stream water concentrations of dissolved organic matter (DOM) and those calculated with the model assuming constant k_p', k_{sr}, and k_{rem} (dashed line) and temperature-dependent k_{sr} and k_{rem} (solid line).

discharge associated with base flow conditions increased gradually throughout the 2 month period, it remained relatively low at level less than 0.03 mm h^{-1}.

4.1.2. Stream Water DOM Dynamics

[36] Storm event peaks in DOM concentration ranged from 4.5 mg C L^{-1} to 13.6 mg C L^{-1} during the fall 2010 time period (Figure 5b). Peak stream water DOM concentrations were lower than DOM concentrations measured in waters from the soil lysimeters (11 to 35 mg C L^{-1}), but were much higher than groundwater DOM concentrations (1 ± 0.5 mg C L^{-1}). The temporal variation of stream water DOM qualitatively resembled the temporal changes in discharge: DOM concentrations increased on the rising limb of the hydrograph, reached a peak value within two hours of peak discharge, and decreased on the falling limb of the hydrograph, although at a slower rate than stream discharge (Figures 5a and 5b). Concentrations of DOM associated with base flow conditions decreased from 3.3 mg C L^{-1} in early October to 1.8 mg C L^{-1} in early December. The DOM mass exported during stormflow comprised 77% of total DOM exported over the 2 month time frame, while the mass exported during stream base flow accounted for the remaining 23% of the total.

4.2. Simulation of Streamflow: Calibration to Fall 2010 Data

[37] Initial analyses of the rainfall-runoff model involved evaluating the appropriateness of single-valued (nonhysteretic) functions of discharge sensitivity ($g(Q)$) for approximating time series measurements of streamflow. Several single-valued $g(Q)$ functions were tested, including a power law relationship; piecewise linear functions; piecewise linear-in-logs functions; and the quadratic-in-logs function as employed by *Kirchner* [2009] to describe streamflow within headwater catchments of mid-Wales. Versions of the rainfall-runoff formulation that incorporated the nonhysteretic $g(Q)$ functions reproduced the timing and, in some cases, the magnitude of peak flows during rainfall events, but consistently underestimated the rate of hydrograph recession. The overall model data mismatch was considerable, such that computations of the Nash-Sutcliffe efficiency (R^2) did not exceed 0.05 for any of the single-valued $g(Q)$ functions tested. One interpretation for the poor agreement between measured and modeled discharge is that rate of change of discharge with catchment water storage is greater during catchment drainage than catchment imbibition.

[38] Accounting for hysteresis in the $g(Q)$ function by using equations (5)–(7) in the rainfall-runoff model improved agreement between simulated and observed stream discharges substantially (Figure 5a). Although this version of the model fails to capture all the variation in the measured discharge hydrograph, the R^2 value for the model fit equals 0.7 and is at least fourteenfold greater than R^2 values associated with simulations that did not account for Q-S hysteresis. Furthermore, the indices that quantify the goodness of model description of storm event peak discharges and export volumes exceed 0.75 (Table 1). The model solution also matches the rate of discharge recession to base flow, which is the characteristic of the observed hydrograph most poorly described by forms of the model governed by single-valued Q-S functions.

[39] The model inversion involved adjusting the parameters of the Q-S relationship to match the stream hydrograph data. The best fit estimates of m_i, the discharge sensitivity during imbibition, is approximately an order of magnitude less than m_{fd}, the discharge sensitivity during fast-recession drainage (Table 1), demonstrating the hysteretic nature of the discharge-storage relationship for the Bigelow Brook catchment. The value for m_{bd}, the discharge sensitivity during base flow drainage, is an order of magnitude smaller than m_i, indicating that, as discharge drops below a threshold that approximates the return to base flow conditions (i.e., Q_{anc}), streamflow becomes less sensitive to changes in catchment water storage.

[40] Model computations of catchment water storage (S) vary by 80 mm over the course of the 2 month simulation (Figure 6). Catchment water storage rises rapidly upon the onset of rainfall, and declines more gradually than stream discharge following the cessation of rainfall. Although calculated S fluctuates considerably, an increasing trend is readily apparent, indicating that the catchment gains water during the simulation time frame. The temporal patterns of simulated storage mimic water table fluctuations measured in the toe slope groundwater well, but exhibit greater amplitude than water table fluctuations recorded in the upland well (compare Figures 6a and 6b). The similarity between modeled results and those measured in the toe slope well suggest that the modeled S is realistic; however, close reproduction of observations should not be expected because the simulated results represent some catchment-averaged storage, while the well measurements correspond to points within the catchment.

[41] The time-evolving Q-S relationship (Figure 7) illustrates how a specific value of S may be associated with various values of Q. Hysteresis occurs in a clockwise direction such that discharge during catchment wetting is larger than that during catchment drainage for the same level of water storage S. The slope of the Q-S relationship is much steeper on the fast recession limb than the rising limb. For separate rainfall events, the Q-S loops are triangles that "slide" along and above the single-valued line for the base flow Q-S relationship. The positions of the triangles depend on the initial water storage at the onset of imbibition, and the sizes of the triangles are determined by the magnitude of the precipitation event.

4.3. Simulation of Stream Water DOM Dynamics: Calibration to Fall 2010 Data

[42] The agreement between the model-simulated results and the high temporal resolution measurements of stream water DOM concentrations is reasonably good (Figure 5b, dashed line and symbols). The R^2 for the overall goodness of model fit to the data equals 0.73. Calculations of GOP_C and GOM_C reveal that the model approximates the peak

Table 1. Best Fit Parameter Values, Standard Errors (SE) of the Parameter Estimates, and Values of Goodness-of-Fit Indices

Rainfall-Runoff Model			DOM Model		
Parameters	Best Fit Values	SE	Parameters	Best Fit Values	SE
m_i (h^{-1})	7×10^{-3}	9×10^{-4}	k'_p (L mg C^{-1})	0.0345	0.6×10^{-4}
m_{fd} (h^{-1})	0.1	0.003	k_{sr} (mg C L^{-1} h^{-1})	0.0923	0.6×10^{-4}
m_{bd} (h^{-1})	3×10^{-4}	5×10^{-5}	k_{rem} (h^{-1})	0.0390	0.7×10^{-4}
k_E	0.81	0.03			

	Rainfall-Runoff Model		DOM Model	
	Calibration	Test	Calibration	Test
Goodness of Fit	Oct–Nov 2010	Oct 2009	Oct–Nov 2010	Oct 2009
R^2	0.70	0.60	0.73	0.76
GOP	0.81	0.83	0.84	0.78
GOM	0.78	0.62	0.72	0.75

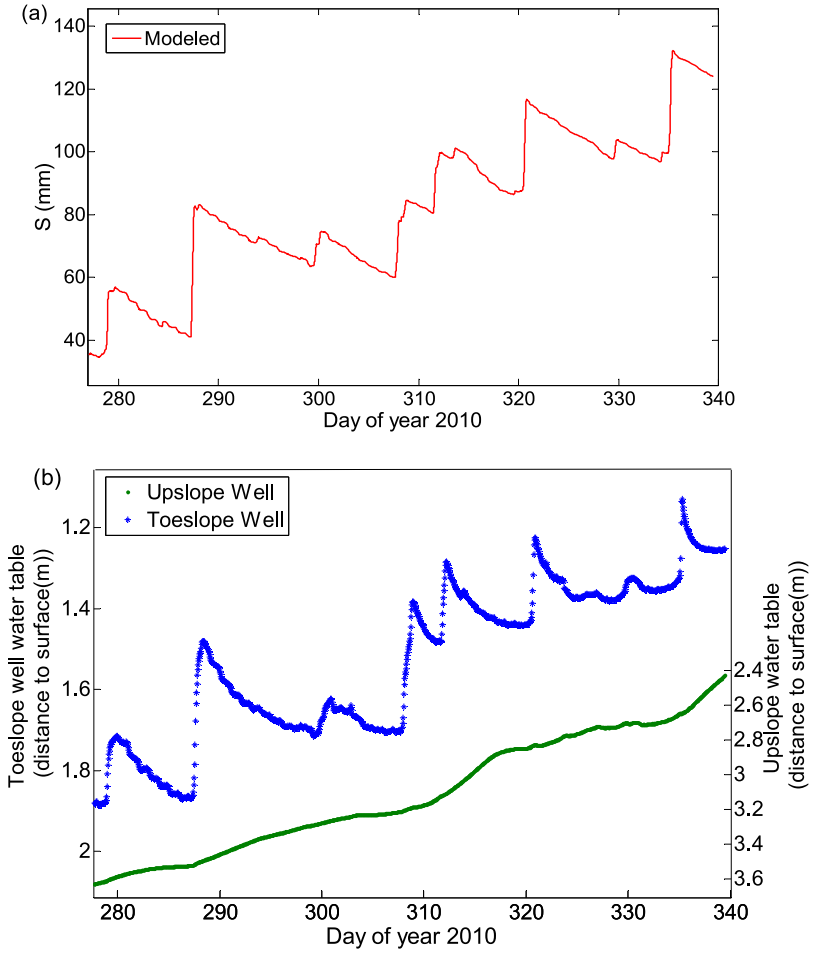

Figure 6. (a) Model computations of catchment-averaged storage, *S*, and (b) measurements of groundwater levels made at the toe slope and upslope locations of Bigelow Brook watershed.

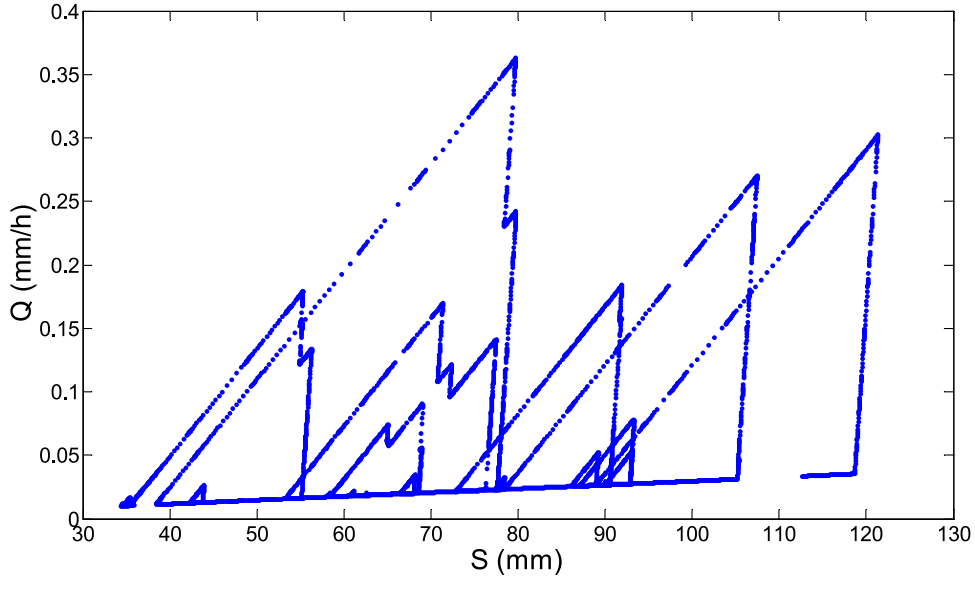

Figure 7. Time-evolving relationship between *Q* and *S* during October and November 2010 in Bigelow Brook watershed.

values of DOM concentration that occur during rainfall events and storm event mass export of DOM with good success (Table 1). The largest discrepancy between modeled and observed results are associated with the period of base flow recession, when the model slightly underestimates stream water DOM concentrations during the early stages of the simulation and overestimates DOM stream water concentrations during the later stages of the simulation.

[43] The values of k_p', k_{sr}, and k_{rem} associated with the best model fit to stream water DOM data are 0.034 L mg C^{-1}, 0.092 mg C L^{-1} h^{-1}, and 0.039 h^{-1}, respectively (Table 1). Conditional simulations show that k_p', which governs rapid dissolution of a readily soluble organic matter, controls the magnitude of the peaks in DOM concentration that occur during rainfall (Figure 8a). The coefficients that govern rate-limited DOM production (k_{sr}) and consumption (k_{rem}) exert comparatively little influence on the model solution during periods in which stream water DOM concentrations change rapidly, but are important in regulating stream water DOM concentrations during periods of stream base flow (Figures 8b and 8c). As rainfall occurs frequently throughout the simulation time frame, periods of uninterrupted base flow are short, typically lasting less than 10 days. If base flow conditions were sustained for greater periods of time (owing to the absence of rainfall), stream water DOC concentrations would vary smoothly with gradually declining catchment water storage and with a rate of change governed by the competing kinetics processes of DOC release (as quantified by k_{sr}) and DOC removal (as quantified by k_{rem}).

4.4. Testing the Calibrated Model Against Fall 2009 Data

[44] Using parameters estimated from the 2010 calibration period, the model captures much of the temporal variations in stream discharge and DOM concentrations recorded during fall 2009 (Figures 9a and 9b and Table 1). The model mimics the timing of the rising limbs of the storm event hydrographs and generally reproduces the magnitude of the peak flows, but underestimates the volume of water exported from the watershed during the second and last storm events of October 2009 (Figure 9a). These discrepancies reflect, to some degree, deficiencies in the structure of the rainfall-runoff formulation that arise from our attempts to simplify complex hydrological processes. Inaccuracies in specification of rainfall amounts, which were estimated from a rain gauge located 1.5 m outside of the watershed, may also contribute to the deviations between measured and modeled discharge. The underestimation of stream discharge during the second and last rainfall events of October 2009 causes the model to underestimate peak concentrations of stream water DOM during these times (Figure 9b). Nevertheless, this mismatch is not substantial and occurs over a small portion of the simulation period and hence the model captures nearly 80% of the variation in the measured DOM data (Table 1).

5. Discussion

5.1. Streamflow Fluctuations

[45] The reasonably good agreement between measured and simulated stream discharges suggests that streamflow dynamics at Bigelow Brook can be approximated by a model that uses observations of rainfall and evapotranspiration as input into conservation-of-mass statement formulated under the assumption that stream discharge is function of catchment-averaged water storage. This assumption has been employed extensively in published research on rainfall-runoff estimation [*Dooge*, 1959; *Laurenson*, 1964; *Rodriguez-Iturbe and Valdes*, 1979; *Wooding*, 1997], and was recently used by *Kirchner* [2009] as a part of a novel approach that eliminates constraints on the functional form of the *Q*-*S* relationship, allowing it to be determined directly from the rainfall-runoff data for a particular catchment. The model presented here builds on the approach of *Kirchner* [2009] by introducing a hysteretic *Q*-*S* function. Hysteresis in the relationship between *Q* and *S* has been observed in many, but certainly not all, headwater catchments [*Myrabo*, 1997; *Kendall et al.*, 1999; *Norbiato and Borga*, 2008; *Graham et al.*, 2010], and our analysis revealed that its consideration was necessary to reproduce measured streamflow fluctuations within the Bigelow Brook watershed.

[46] We adopted a three-segment, piecewise linear function to describe hysteresis in the *Q*-*S* relationship and estimated the slopes of these linear segments through model calibration. Although application of this piecewise linear function does not restrict the direction of hysteresis, the best fit parameterization for Bigelow Brook indicated that *Q*-*S* hysteresis was clockwise. This clockwise hysteresis mirrors observations from several watersheds, including the HJA experimental forest watershed in the western Cascades, Oregon [*Graham et al.*, 2010], and Sleepers River research watershed in northeastern Vermont [*McDonnell et al.*, 1998]. Some watersheds, in contrast, exhibit counterclockwise hysteresis such that stream discharge for a given catchment storage is greater during catchment drainage than imbibition [e.g., *Hrncir et al.*, 2010]. This range in watershed response behaviors poses a challenge to streamflow prediction and reflects differences in catchment geology, topography, geomorphology, and climate, which, in turn, lead to differences in the primary mechanisms of surface and subsurface runoff and the way they contribute to streamflow.

[47] The hysteretic function used for simulating streamflow fluctuations at Bigelow Brook is simple, particularly with respect to representation of the *Q*-*S* relationship for catchment imbibition. According to the formulation, the discharge response to increases in catchment storage is linear (as quantified by m_i) and independent of the amount of water held in storage at the onset of a rainfall event. This relationship is not universally applicable and its appropriateness here may be attributable to the moderate variations in catchment storage that occurred during the 2 month simulation. Rainfall during this period totaled 225 mm and was distributed over eight storms, inducing a 100 mm range in catchment-averaged water storage (Figure 6a). Over a greater range in storage, nonlinearity and sensitivity to antecedent wetness may emerge as defining characteristics of the *Q*-*S* relationship for imbibition of the Bigelow Brook Watershed. While not observed in this work, these complicating factors have been reported in other studies of runoff formation [*Harman and Sivapalan*, 2009; *Spence et al.*, 2010; *Teuling et al.*, 2010; *Ajami et al.*, 2011], and could be accounted for in the present

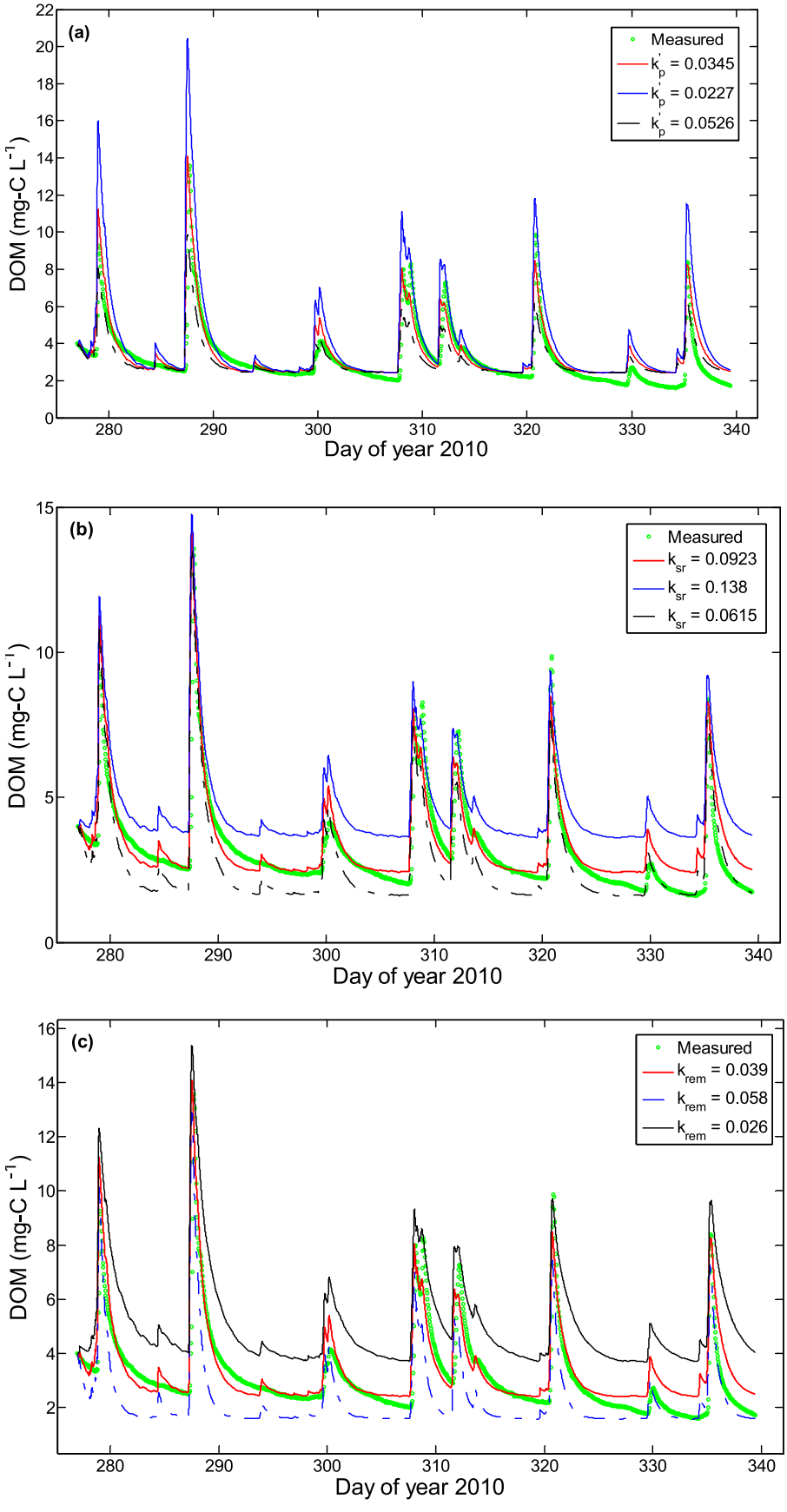

Figure 8. Sensitivity of model-simulated, stream water DOM concentrations to changes values of (a) k_p', (b) k_{sr}, and (c) k_{rem}. The red lines were calculated with best fit parameter values, and the green and blue lines were calculated by perturbing the best fit values by 50%.

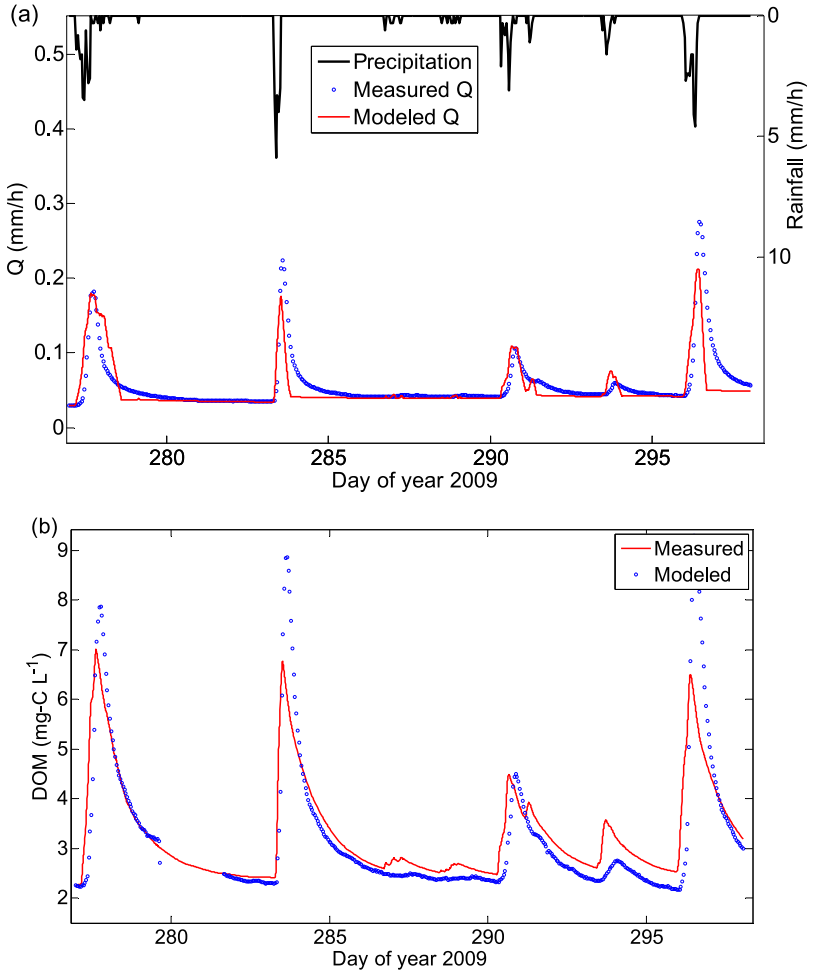

Figure 9. Field observations and model simulations for fall 2009: (a) measurements of precipitation and stream discharge and model calculations of stream discharge and (b) measurements and model calculations of stream water DOM concentrations.

model framework by replacing equations (5)–(7) with alternative formulations.

[48] The slopes of the linear segments of the *Q*-*S* function define the storage rate of change in discharge and hence can be viewed as the efficiency in which the watershed coverts changes in terrestrial water storage to changes in stream discharge [*Spence*, 2007]. The segment slopes of the best fit *Q*-*S* function for Bigelow Brook equal 7×10^{-3} and 3×10^{-4} h^{-1} for imbibition and base flow drainage, respectively, indicating that the catchment is 23 times more efficient in transmitting water to the stream during periods of rainfall than during periods of stream base flow. Between catchment imbibition and base flow discharge drops precipitously for an incremental change in catchment storage (Figure 7), which is suggestive of threshold type or a switching behavior [*Tromp-van Meerveld and McDonnell*, 2006; *O'Kane and Flynn*, 2007; *Zehe and Sivapalan*, 2009; *Detty and McGuire*, 2010].

[49] Consideration of the overall characteristics of the best fit *Q*-*S* function in light of published interpretations of rainfall-runoff processes [*Devito et al.*, 1996; *Jencso et al.*, 2009; *McGuire and McDonnell*, 2010; *Spence et al.*, 2010] seems to imply that streamflow fluctuations at Bigelow Brook are governed by changes in the connectivity of subsurface flow paths, which, in turn, are regulated by variations in the amount of water stored within the catchment. At Bigelow Brook, increases in storage that occur following the onset of precipitation must promote the connection of shallow subsurface flow paths with relatively high permeability. These flow paths gain connectivity quickly and thus are likely to form in riparian areas that drain convergent portions of the catchment's hill slopes and that remain on the verge of saturation or are prone to perched saturation. It is the transmission of water through the shallow, near-streamflow paths that dominate stream quick flow response to rainfall. Only a fraction of the incident rainwater is conducted through shallow, near-streamflow paths and to the stream and hence catchment-averaged storage increases throughout the rainfall event. Upon the cessation of rainfall, incremental reductions in watershed storage lead to a loss in the lateral connectivity of permeable, shallow flow paths, causing stream discharge to drop precipitously as flow toward the stream is relegated to deeper subsurface flow paths that transmit water more slowly. This

cycle is completed and the formation a new hysteresis loop begins with the onset of the next rainfall event.

5.2. Stream Water DOM Dynamics

[50] Models for quantifying the concentrations and fluxes of DOM from land to streams vary from simple regressions [*Creed et al.*, 2008; *Agren et al.*, 2010] to more elaborate process-based formulations [*Grieve*, 1991; *Hornberger et al.*, 1994; *Boyer et al.*, 1996; *Canham et al.*, 2004; *Futter et al.*, 2007; *Yurova et al.*, 2008; *Jutras et al.*, 2011; *Schelker et al.*, 2011]. In all the process-based models, including the one presented in this study, the dynamics of DOM are governed by production, consumption, retention, and leaching. The models differ, however, by number of pools and forms of terrestrial carbon considered; the level of detail use to simulate the amounts and transformations of carbon; and the way in which carbon biogeochemistry is coupled to hydrologic routing. Our model is comparable in the level of structural and parametric complexity to those developed by *Grieve* [1991], *Hornberger et al.* [1994], and *Boyer et al.* [1996], but treats terrestrial carbon biogeochemistry at a much lower level of detail than INCA-C [*Futter et al.*, 2007] and published ecosystem and soil carbon models, including DyDOC [*Michalzik et al.*, 2003] and the DOC synthesis model [*Neff and Asner*, 2001], which is based on the CENTURY framework [*Parton et al.*, 1988]. There are exceedingly few published evaluations of models against data on stream water DOM export [*Boyer et al.*, 1996; *Futter et al.*, 2007; *Hornberger et al.*, 1994], particularly during rainfall and snowmelt periods when DOM fluxes are especially high, and those that are available suggest that continued improvement of frameworks for stream water DOM fluctuations are in order. The DOM mixing and reaction model that is coupled to the rainfall-runoff model reproduces 73% and 76% of the hourly variations in stream water DOM concentrations in fall 2010 and fall 2009, respectively. The simply formulated model is capable of describing the timing and magnitude of event-based DOM peaks, the fast decline after precipitation ceases, and the moderate tailing under base flow conditions. The good match between the modeled and measured DOM time series suggests that our model provides a reasonable approximation of the coupled hydrological and biogeochemical controls on DOM export from Bigelow Brook.

[51] Our model results demonstrate an important linkage of carbon export to fluctuations in catchment water storage. This finding is in line with previous DOM studies in forested watershed [*Hornberger et al.*, 1994; *Boyer et al.*, 1996; *Brown et al.*, 1999; *Hagedorn et al.*, 2000; *Inamdar and Mitchell*, 2006], reflecting the correspondence between increasing stream water DOM concentrations and the catchment water level rise. This correspondence is not universal, however, as in some watersheds with permeable geologic media that permits deep percolation, stream DOM concentrations are not be related to water table fluctuations [*Moore et al.*, 2003].

[52] It is our hypothesis that the DOM appearing in the stream during rainfall events at Bigelow Brook is derived mainly from the riparian zone. Our soil lysimeter data show DOM concentrations in shallow soil horizons are as high as 92 mg C L^{-1} after a dry summer period in riparian locations, which is nearly 90 times greater than DOM concentrations measured in water samples taken from the upslope groundwater well. The quick flow response that is dominated by the transmission of water through shallow, near-streamflow paths (as discussed above) is consistent with the hypothesis that the riparian zone is the principal source of stream DOM during stormflow periods. In glaciated watersheds with moderate topography similar to Bigelow Brook, riparian soils have been demonstrated to be the dominant sources of DOM [*Hemond*, 1990; *Hinton et al.*, 1998]. In a small catchment with 8 to 30% topographic gradient in central Ontario, Canada, *Hinton et al.* [1998] demonstrated that riparian zone (within 5–25 m of the stream channel) soils contributed 73–84% of the stream DOM export during an autumn storm. Although our DOM model is a catchment-averaged model, the well-mixed reservoir assumption works reasonably well probably because the observed stream water DOM dynamics are most sensitive to processes that occur within a small part of the catchment very near the stream [*Fiebig et al.*, 1990; *Hinton et al.*, 1998; *McGlynn and McDonnell*, 2003b]. Less parsimonious model formulations that relax the well-mixed reservoir assumption or that account for contributions from multiple subsurface reservoirs may be required to simulate stream water DOC concentrations in larger watersheds or in cases in which storm event responses are significantly influenced by the delivery of solutes and water from upland areas to the stream.

[53] The carbon model involves calibrating three biogeochemical parameters: the lumped coefficients for the instantaneous release (k_p'), rate-limited DOM release (k_{sr}), and removal by adsorption and biodegradation (k_{rem}). Although suitable for our study, the assumption that terrestrial carbon biogeochemistry can be approximated with a model that uses constant-valued coefficients may be inappropriate for simulating DOM dynamics at interseasonal and longer time scales. The processes of DOM generation and consumption vary with several factors, including temperature [*Liechty et al.*, 1995; *Kalbitz et al.*, 2000; *Lumsdon et al.*, 2005]. In our study, observed DOM concentrations are consistently overestimated by the model as daily temperatures decreased during the latter half of the simulation period (Figure 5b, compare circles and dashed line). Kinetics coefficients that quantify biogeochemical reactions are often reported to vary with temperature in a power law or exponential fashion [*Cornelissen et al.*, 1997; *Sparks*, 2003]. By expressing values of the rate coefficients (k_{sr} and k_{rem}) in an even simpler fashion, as linear functions of average daily temperature, we are able to narrow the discrepancies between observed and modeled DOM concentrations between days 310 and 340 of the simulation (Figure 5b, compare circles and solid line). The processes governing DOM production and consumption are undoubtedly sensitive to other factors, in addition to temperature, that affect the size and composition of the soil organic matter pool. These factors include, for example, soil moisture, seasonally dependent inputs of fresh organic matter by leaf litter fall and root exudation, and the extent to which the soil organic matter pool has been altered by abiotic and biotic processes [*Findlay and Sinsabaugh*, 2002; *Dawson et al.*, 2008]. For periods that stretch beyond a season, we anticipate that our assumptions of constant model coefficients and soil carbon pool size will fail, and thus, our approach will have to be

extended to account for more sophisticated treatments of terrestrial carbon biogeochemistry, such as those used in INCA-C or ecosystem models [*Neff and Asner*, 2001; *Michalzik et al.*, 2003; *Futter et al.*, 2007]. In particular, these extensions may involve expressing the coefficients that govern DOC production and consumption (k'_p, k_{sr}, and k_{rem} in equation (17)) as linear or nonlinear functions of catchment water storage (as a surrogate for soil wetness) in addition to soil temperature and by accounting for variations in the size of the soil carbon pool by introducing additional equations that describe temporal changes in concentrations of solid organic matter due to processes such as litter fall, root breakdown, dissolution, and adsorption of DOC.

6. Summary and Conclusions

[54] The punctuated response of stream water DOM concentrations to rainfall and the synchronized variations of DOM and stream discharge are widely observed [*Raymond and Saiers*, 2010]. We present a physically based model intended to capture the principal characteristics of this response. This model links a rainfall-runoff formulation that accounts for hysteresis in the discharge-storage relationship with a soil water carbon model that treats the processes of soil water DOM production and consumption as time-dependent, catchment-averaged processes. Comparison of model calculations to field measurements reveal a tight coupling between changes in catchment-averaged water storage and the mass of DOM delivered to the stream from the terrestrial landscape. This model represents a simple framework for quantifying key processes dominating event-driven DOM export from small, forested watersheds. As such, it may be applicable to at least some of the many other watersheds that exhibit similar rainfall-runoff behavior and DOM-export responses.

[55] **Acknowledgments.** We are grateful for the assistance of Harvard Forest staff, especially Emery Boose, for providing the stream discharge and meteorological data. The comments of the Associate Editor and three reviewers were especially helpful in improving the manuscript. This research was supported through the Schlumberger Foundation Faculty for the Future Fellowship awarded to Na Xu, Yale Institute for Biospheric Studies Environmental Fellowship awarded to Henry Wilson, and Department of Energy grant DE-F602-08ER6463 and National Science Foundation grant EAR1014478 awarded to James Saiers.

References

Agren, A., I. Buffam, K. Bishop, and H. Laudon (2010), Modeling stream dissolved organic carbon concentrations during spring flood in the boreal forest: A simple empirical approach for regional predictions, *J. Geophys. Res.*, *115*, G01012, doi:10.1029/2009JG001013.

Ajami, H., P. A. Troch, T. Maddock III, T. Meixner, and C. Eastoe (2011), Quantifying mountain block recharge by means of catchment-scale storage-discharge relationships, *Water Resour. Res.*, *47*, W04504, doi:10.1029/2010WR009598.

Allen, R. G., L. S. Pereira, D. D. Raes, and M. Smith (1998), Crop evapotranspiration, guidelines for computing crop water requirements, *FAO Irrig. Drain. Pap. 56*, pp. 1–15, Food and Agric. Organ., Rome.

Austnes, K., C. D. Evans, C. Eliot-Laize, P. S. Naden, and G. H. Old (2010), Effects of storm events on mobilisation and in-stream processing of dissolved organic matter (DOM) in a Welsh peatland catchment, *Biogeochemistry*, *99*(1–3), 157–173, doi:10.1007/s10533-009-9399-4.

Bathurst, J. C. (1986), Physically-based distributed modeling of an upland catchment using the Systeme Hydrologique Europeen, *J. Hydrol.*, *87*(1–2), 79–102, doi:10.1016/0022-1694(86)90116-2.

Bertotti, G., and I. D. Mayergoyz (2006), *The Science of Hysteresis*, Academic, Amsterdam.

Beven, K. (2006), Searching for the holy grail of scientific hydrology: $Q_t = H(S\leftarrow, R\leftarrow, \Delta t)$ A as closure, *Hydrol. Earth Syst. Sci.*, *10*(5), 609–618.

Bishop, K. H., H. Laudon, and S. Kohler (2000), Separating the natural and anthropogenic components of spring flood pH decline: A method for areas that are not chronically acidified, *Water Resour. Res.*, *36*(7), 1873–1884, doi:10.1029/2000WR900030.

Boone, R. D. (1994), Light-fraction soil organic-matter—Origin and contribution to net nitrogen mineralization, *Soil Biol. Biochem.*, *26*(11), 1459–1468, doi:10.1016/0038-0717(94)90085-x.

Borken, W., E. A. Davidson, K. Savage, E. T. Sundquist, and P. Steudler (2006), Effect of summer throughfall exclusion, summer drought, and winter snow cover on methane fluxes in a temperate forest soil, *Soil Biol. Biochem.*, *38*(6), 1388–1395, doi:10.1016/j.soilbio.2005.10.011.

Boyer, E. W., G. M. Hornberger, K. E. Bencala, and D. McKnight (1996), Overview of a simple model describing variation of dissolved organic carbon in an upland catchment, *Ecol. Modell.*, *86*(2–3), 183–188, doi:10.1016/0304-3800(95)00049-6.

Boyer, E. W., G. M. Hornberger, K. E. Bencala, and D. M. Mcknight (1997), Response characteristics of DOC flushing in an alpine catchment, *Hydrol. Processes*, *11*(12), 1635–1647.

Brooks, P. D., D. M. McKnight, and K. E. Bencala (1999), The relationship between soil heterotrophic activity, soil dissolved organic carbon (DOC) leachate, and catchment-scale DOC export in headwater catchments, *Water Resour. Res.*, *35*(6), 1895–1902, doi:10.1029/1998WR900125.

Brown, V. A., J. J. McDonnell, D. A. Burns, and C. Kendall (1999), The role of event water, a rapid shallow flow component, and catchment size in summer stormflow, *J. Hydrol.*, *217*(3–4), 171–190.

Buffam, I., J. N. Galloway, L. K. Blum, and K. J. McGlathery (2001), A stormflow/baseflow comparison of dissolved organic matter concentrations and bioavailability in an Appalachian stream, *Biogeochemistry*, *53*(3), 269–306.

Canham, C. D., M. L. Pace, M. J. Papaik, A. G. B. Primack, K. M. Roy, R. J. Maranger, R. P. Curran, and D. M. Spada (2004), A spatially explicit watershed-scale analysis of dissolved organic carbon in Adirondack lakes, *Ecol. Appl.*, *14*(3), 839–854.

Chorover, J., and M. K. Amistadi (2001), Reaction of forest floor organic matter at goethite, birnessite and smectite surfaces, *Geochim. Cosmochim. Acta*, *65*(1), 95–109.

Chow, A. T., K. K. Tanji, and S. D. Gao (2003), Production of dissolved organic carbon (DOC) and trihalomethane (THM) precursor from peat soils, *Water Res.*, *37*(18), 4475–4485.

Collins, B. M., W. V. Sobczak, and E. A. Colburn (2007), Subsurface flowpaths in a forested headwater stream harbor a diverse macroinvertebrate community, *Wetlands*, *27*(2), 319–325.

Cornelissen, G., P. C. M. VanNoort, J. R. Parsons, and H. A. J. Govers (1997), Temperature dependence of slow adsorption and desorption kinetics of organic compounds in sediments, *Environ. Sci. Technol.*, *31*(2), 454–460.

Creed, I. F., F. D. Beall, T. A. Clair, P. J. Dillon, and R. H. Hesslein (2008), Predicting export of dissolved organic carbon from forested catchments in glaciated landscapes with shallow soils, *Global Biogeochem. Cycles*, *22*, GB4024, doi:10.1029/2008GB003294.

Currie, W. S., J. D. Aber, W. H. McDowell, R. D. Boone, and A. H. Magill (1996), Vertical transport of dissolved organic C and N under long-term n amendments in pine and hardwood forests, *Biogeochemistry*, *35*(3), 471–505.

Dawson, J. J. C., C. Soulsby, D. Tetzlaff, M. Hrachowitz, S. M. Dunn, and I. A. Malcolm (2008), Influence of hydrology and seasonality on DOC exports from three contrasting upland catchments, *Biogeochemistry*, *90*(1), 93–113.

Detty, J. M., and K. J. McGuire (2010), Threshold changes in storm runoff generation at a till-mantled headwater catchment, *Water Resour. Res.*, *46*, W07525, doi:10.1029/2009WR008102.

Devito, K. J., A. R. Hill, and N. Roulet (1996), Groundwater-surface water interactions in headwater forested wetlands of the Canadian Shield, *J. Hydrol.*, *181*(1–4), 127–147, doi:10.1016/0022-1694(95)02912-5.

Dooge, J. C. I. (1959), A general theory of the unit hydrograph, *J. Geophys. Res.*, *64*(2), 241–256, doi:10.1029/JZ064i002p00241.

Duarte, C. M., and Y. T. Prairie (2005), Prevalence of heterotrophy and atmospheric CO_2 emissions from aquatic ecosystems, *Ecosystems*, *8*(7), 862–870, doi:10.1007/s10021-005-0177-4.

Dunnivant, F. M., P. M. Jardine, D. L. Taylor, and J. F. McCarthy (1992), Cotransport of cadmium and hexachlorobiphenyl by dissolved

organic-carbon through columns containing aquifer material, *Environ. Sci. Technol.*, *26*(2), 360–368.

Easthouse, K. B., J. Mulder, N. Christophersen, and H. M. Seip (1992), Dissolved organic-carbon fractions in soil and stream water during variable hydrological conditions at Birkenes, southern Norway, *Water Resour. Res.*, *28*(6), 1585–1596, doi:10.1029/92WR00056.

Ewen, J., and S. J. Birkinshaw (2007), Lumped hysteretic model for subsurface stormflow developed using downward approach, *Hydrol. Processes*, *21*(11), 1496–1505, doi:10.1002/hyp.6344.

Fiebig, D. M., M. A. Lock, and C. Neal (1990), Soil water in the riparian zone as a source of carbon for a headwater stream, *J. Hydrol.*, *116*(1–4), 217–237.

Findlay, S., and R. L. Sinsabaugh (Eds.) (2002), *Aquatic Ecosystems: Interactivity of Dissolved Organic Matter*, Academic, San Diego, Calif.

Futter, M. N., D. Butterfield, B. J. Cosby, P. J. Dillon, A. J. Wade, and P. G. Whitehead (2007), Modeling the mechanisms that control in-stream dissolved organic carbon dynamics in upland and forested catchments, *Water Resour. Res.*, *43*, W02424, doi:10.1029/2006WR004960.

Graham, C. B., W. van Verseveld, H. R. Barnard, and J. J. McDonnell (2010), Estimating the deep seepage component of the hillslope and catchment water balance within a measurement uncertainty framework, *Hydrol. Processes*, *24*(25), 3631–3647, doi:10.1002/hyp.7788.

Green, I. R. A., and D. Stephenson (1986), Criteria for comparison of single event models, *Hydrol. Sci. J.*, *31*(3), 395–411.

Grieve, I. C. (1991), A model of dissolved organic carbon concentrations in soil and stream waters, *Hydrol. Processes*, *5*(3), 301–307.

Guggenberger, G., B. Glaser, and W. Zech (1994), Heavy-metal binding by hydrophobic and hydrophilic dissolved organic-carbon fractions in a Spodosol A and B horizon, *Water Air Soil Pollut.*, *72*(1–4), 111–127.

Guggenberger, G., K. Kaiser, and W. Zech (1998), Mobilization and immobilization of dissolved organic matter in forest soils, *Z. Pflanzenernahrung Bodenkd.*, *161*(4), 401–408.

Hagedorn, F., P. Schleppi, P. Waldner, and H. Fluhler (2000), Export of dissolved organic carbon and nitrogen from gleysol dominated catchments—The significance of water flow paths, *Biogeochemistry*, *50*(2), 137–161.

Harman, C., and M. Sivapalan (2009), A similarity framework to assess controls on shallow subsurface flow dynamics in hillslopes, *Water Resour. Res.*, *45*, W01417, doi:10.1029/2008WR007067.

Hemond, H. F. (1990), Wetlands as the source of dissolved organic carbon to surface waters, in *Organic Acids in Aquatic Ecosystems*, edited by E. Perdue and E. Gjessing, pp. 301–313, John Wiley, New York.

Hinton, M. J., S. L. Schiff, and M. C. English (1998), Sources and flowpaths of dissolved organic carbon during storms in two forested watersheds of the Precambrian shield, *Biogeochemistry*, *41*(2), 175–197, doi:10.1023/a:1005903428956.

Hongve, D. (1999), Production of dissolved organic carbon in forested catchments, *J. Hydrol.*, *224*(3–4), 91–99.

Hood, E., M. N. Gooseff, and S. L. Johnson (2006), Changes in the character of stream water dissolved organic carbon during flushing in three small watersheds, Oregon, *J. Geophys. Res.*, *111*, G01007, doi:10.1029/2005JG000082.

Hope, D., M. F. Billett, and M. S. Cresser (1994), A review of the export of carbon in river water—Fluxes and processes, *Environ. Pollut.*, *84*(3), 301–324.

Hornberger, G. M., K. E. Bencala, and D. M. McKnight (1994), Hydrological controls on dissolved organic-carbon during snowmelt in the Snake River near Montezuma, Colorado, *Biogeochemistry*, *25*(3), 147–165.

Hrncir, M., M. Sanda, A. Kulasova, and M. Cislerova (2010), Runoff formation in a small catchment at hillslope and catchment scales, *Hydrol. Processes*, *24*(16), 2248–2256, doi:10.1002/hyp.7614.

Ikhouane, F., and J. Rodellar (2007), *Systems With Hysteresis: Analysis, Identification and Control Using the Bouc-Wen Model*, Wiley-Interscience, New York.

Inamdar, S. P., and M. J. Mitchell (2006), Hydrologic and topographic controls on storm-event exports of dissolved organic carbon (DOC) and nitrate across catchment scales, *Water Resour. Res.*, *42*, W03421, doi:10.1029/2005WR004212.

Inamdar, S. P., and M. J. Mitchell (2007), Storm event exports of dissolved organic nitrogen (DON) across multiple catchments in a glaciated forested watershed, *J. Geophys. Res.*, *112*, G02014, doi:10.1029/2006JG000309.

Inamdar, S. P., S. F. Christopher, and M. J. Mitchell (2004), Export mechanisms for dissolved organic carbon and nitrate during summer storm events in a glaciated forested catchment in New York, USA, *Hydrol. Processes*, *18*(14), 2651–2661, doi:10.1002/hyp.5572.

Inamdar, S. P., N. O'Leary, M. J. Mitchell, and J. T. Riley (2006), The impact of storm events on solute exports from a glaciated forested watershed in western New York, USA, *Hydrol. Processes*, *20*(16), 3423–3439.

Jencso, K. G., B. L. McGlynn, M. N. Gooseff, S. M. Wondzell, K. E. Bencala, and L. A. Marshall (2009), Hydrologic connectivity between landscapes and streams: Transferring reach-and plot-scale understanding to the catchment scale, *Water Resour. Res.*, *45*, W04428, doi:10.1029/2008WR007225.

Jutras, M. F., et al. (2011), Dissolved organic carbon concentrations and fluxes in forest catchments and streams: DOC-3 model, *Ecol. Modell.*, *222*(14), 2291–2313, doi:10.1016/j.ecolmodel.2011.03.035.

Kaiser, K., and W. Zech (1999), Release of natural organic matter sorbed to oxides and a subsoil, *Soil Sci. Soc. Am. J.*, *63*(5), 1157–1166.

Kalbitz, K., S. Solinger, J. H. Park, B. Michalzik, and E. Matzner (2000), Controls on the dynamics of dissolved organic matter in soils: A review, *Soil Sci.*, *165*(4), 277–304.

Kendall, K. A., J. B. Shanley, and J. J. McDonnell (1999), A hydrometric and geochemical approach to test the transmissivity feedback hypothesis during snowmelt, *J. Hydrol.*, *219*(3–4), 188–205.

Kirchner, J. W. (2009), Catchments as simple dynamical systems: Catchment characterization, rainfall-runoff modeling, and doing hydrology backward, *Water Resour. Res.*, *45*, W02429, doi:10.1029/2008WR006912.

Kohler, S. J., I. Buffam, J. Seibert, K. H. Bishop, and H. Laudon (2009), Dynamics of stream water TOC concentrations in a boreal headwater catchment: Controlling factors and implications for climate scenarios, *J. Hydrol.*, *373*(1–2), 44–56, doi:10.1016/j.jhydrol.2009.04.012.

Laudon, H., S. Kohler, and I. Buffam (2004a), Seasonal TOC export from seven boreal catchments in northern Sweden, *Aquat. Sci.*, *66*(2), 223–230, doi:10.1007/s00027-004-0700-2.

Laudon, H., J. Seibert, S. Kohler, and K. Bishop (2004b), Hydrological flow paths during snowmelt: Congruence between hydrometric measurements and oxygen 18 in meltwater, soil water, and runoff, *Water Resour. Res.*, *40*, W03102, doi:10.1029/2003WR002455.

Laurenson, E. M. (1964), *A Catchment Storage Model for Runoff Routing*, Water Res. Found. of Aust., Broadway, NSW, Australia.

Liechty, H. O., E. Kuuseoks, and G. D. Mroz (1995), Dissolved organic-carbon in northern hardwood stands with differing acidic inputs and temperature regimes, *J. Environ. Qual.*, *24*(5), 927–933.

Lumsdon, D. G., M. I. Stutter, R. J. Cooper, and J. R. Manson (2005), Model assessment of biogeochemical controls on dissolved organic carbon partitioning in an acid organic soil, *Environ. Sci. Technol.*, *39*(20), 8057–8063.

Majone, B., A. Bertagnoli, and A. Bellin (2010), A non-linear runoff generation model in small alpine catchments, *J. Hydrol.*, *385*(1–4), 300–312, doi:10.1016/j.jhydrol.2010.02.033.

McClain, M. E., et al. (2003), Biogeochemical hot spots and hot moments at the interface of terrestrial and aquatic ecosystems, *Ecosystems*, *6*(4), 301–312, doi:10.1007/s10021-003-0161-9.

McDonnell, J. J., B. L. McGlynn, K. Kendall, J. Shanley, and C. Kendall (1998), The role of near-stream riparian zones in the hydrology of steep upland catchments, in *Hydrology, Water Resources and Ecology in Headwaters*, edited by K. Kovar et al., pp. 173–180, IAHS Press, Wallingford, Oxfordshire, UK.

McGlynn, B. L., and J. J. McDonnell (2003a), Role of discrete landscape units in controlling catchment dissolved organic carbon dynamics, *Water Resour. Res.*, *39*(4), 1090, doi:10.1029/2002WR001525.

McGlynn, B. L., and J. J. McDonnell (2003b), Quantifying the relative contributions of riparian and hillslope zones to catchment runoff, *Water Resour. Res.*, *39*(11), 1310, doi:10.1029/2003WR002091.

McGuire, K. J., and J. J. McDonnell (2010), Hydrological connectivity of hillslopes and streams: Characteristic time scales and nonlinearities, *Water Resour. Res.*, *46*, W10543, doi:10.1029/2010WR009341.

Michalzik, B., E. Tipping, J. Mulder, J. F. G. Lancho, E. Matzner, C. L. Bryant, N. Clarke, S. Lofts, and M. A. V. Esteban (2003), Modelling the production and transport of dissolved organic carbon in forest soils, *Biogeochemistry*, *66*(3), 241–264.

Moore, T. R., L. Matos, and N. T. Roulet (2003), Dynamics and chemistry of dissolved organic carbon in Precambrian shield catchments and an impounded wetland, *Can. J. Fish. Aquat. Sci.*, *60*(5), 612–623, doi:10.1139/f03-050.

Morris, D. P., H. Zagarese, C. E. Williamson, E. G. Balseiro, B. R. Hargreaves, B. Modenutti, R. Moeller, and C. Queimalinos (1995), The attenuation of solar UV radiation in lakes and the role of dissolved organic carbon, *Limnol. Oceanogr.*, *40*(8), 1381–1391.

Mulholland, P. J., and W. R. Hill (1997), Seasonal patterns in streamwater nutrient and dissolved organic carbon concentrations: Separating catchment flow path and in-stream effects, *Water Resour. Res.*, *33*(6), 1297–1306, doi:10.1029/97WR00490.

Mulholland, P. J., G. V. Wilson, and P. M. Jardine (1990), Hydrogeochemical response of a forested watershed to storms: Effects of preferential flow along shallow and deep pathways, *Water Resour. Res.*, *26*(12), 3021–3036, doi:10.1029/WR026i012p03021.

Munch, J. M., K. U. Totsche, and K. Kaiser (2002), Physicochemical factors controlling the release of dissolved organic carbon from columns of forest subsoils, *Eur. J. Soil Sci.*, *53*(2), 311–320.

Myrabo, S. (1997), Temporal and spatial scale of response area and groundwater variation in till, *Hydrol. Processes*, *11*(14), 1861–1880.

Nash, J. E., and J. V. Sutcliffe (1970), River flow forecasting through conceptual models part I—A discussion of principles, *J. Hydrol.*, *10*(3), 282–290.

Neff, J. C., and G. P. Asner (2001), Dissolved organic carbon in terrestrial ecosystems: Synthesis and a model, *Ecosystems*, *4*(1), 29–48.

Norbiato, D., and M. Borga (2008), Analysis of hysteretic behaviour of a hillslope-storage kinematic wave model for subsurface flow, *Adv. Water Resour.*, *31*(1), 118–131, doi:10.1016/j.advwatres.2007.07.001.

O'Kane, J. P., and D. Flynn (2007), Thresholds, switches and hysteresis in hydrology from the pedon to the catchment scale: A non-linear systems theory, *Hydrol. Earth Syst. Sci.*, *11*(1), 443–459.

Pacific, V. J., K. G. Jencso, and B. L. McGlynn (2009), Variable flushing mechanisms and landscape structure control stream doc export during snowmelt in a set of nested catchments, *Biogeochemistry*, *99*(1–3), 193–211, doi:10.1007/s10533-009-9401-1.

Palmer, S. M., D. Hope, M. F. Billett, J. J. C. Dawson, and C. L. Bryant (2001), Sources of organic and inorganic carbon in a headwater stream: Evidence from carbon isotope studies, *Biogeochemistry*, *52*(3), 321–338.

Parker, J. C., and R. J. Lenhard (1987), A model for hysteretic constitutive relations governing multiphase flow: 1. Saturation-pressure relations, *Water Resour. Res.*, *23*(12), 2187–2196, doi:10.1029/WR023i012p02187.

Parton, W. J., J. W. B. Stewart, and C. V. Cole (1988), Dynamics of C, N, P and S in grassland soils: A model, *Biogeochemistry*, *5*(1), 109–131, doi:10.1007/bf02180320.

Polarski, M. (1997), Distributed rainfall-runoff model incorporating channel extension and gridded digital maps, *Hydrol. Processes*, *11*(1), 1–11, doi:10.1002/(sici)1099-1085(199701)11:1<1::aid-hyp388>3.0.co;2-g.

Raymond, P. A., and J. E. Saiers (2010), Event controlled DOC export from forested watersheds, *Biogeochemistry*, *100*(1–3), 197–209, doi:10.1007/s10533-010-9416-7.

Rodriguez-Iturbe, I., and J. B. Valdes (1979), Geomorphologic structure of hydrologic response, *Water Resour. Res.*, *15*(6), 1409–1420, doi:10.1029/WR015i006p01409.

Saraceno, J. F., B. A. Pellerin, B. D. Downing, E. Boss, P. A. M. Bachand, and B. A. Bergamaschi (2009), High-frequency in situ optical measurements during a storm event: Assessing relationships between dissolved organic matter, sediment concentrations, and hydrologic processes, *J. Geophys. Res.*, *114*, G00F09, doi:10.1029/2009JG000989.

Schelker, J., D. A. Burns, M. Weiler, and H. Laudon (2011), Hydrological mobilization of mercury and dissolved organic carbon in a snow-dominated, forested watershed: Conceptualization and modeling, *J. Geophys. Res.*, *116*, G01002, doi:10.1029/2010JG001330.

Schiff, S. L., R. Aravena, S. E. Trumbore, and P. J. Dillon (1990), Dissolved organic-carbon cycling in forested watersheds: A carbon isotope approach, *Water Resour. Res.*, *26*(12), 2949–2957, doi:10.1029/WR026i012p02949.

Sparks, D. L. (2003), *Environmental Soil Chemistry*, 2nd ed., Academic, San Diego, Calif.

Spence, C. (2007), On the relation between dynamic storage and runoff: A discussion on thresholds, efficiency, and function, *Water Resour. Res.*, *43*, W12416, doi:10.1029/2006WR005645.

Spence, C., X. J. Guan, R. Phillips, N. Hedstrom, R. Granger, and B. Reid (2010), Storage dynamics and streamflow in a catchment with a variable contributing area, *Hydrol. Processes*, *24*(16), 2209–2221, doi:10.1002/hyp.7492.

Teuling, A. J., I. Lehner, J. W. Kirchner, and S. I. Seneviratne (2010), Catchments as simple dynamical systems: Experience from a Swiss prealpine catchment, *Water Resour. Res.*, *46*, W10502, doi:10.1029/2009WR008777.

Tromp-van Meerveld, H. J., and J. J. McDonnell (2006), Threshold relations in subsurface stormflow: 2. The fill and spill hypothesis, *Water Resour. Res.*, *42*, W02411, doi:10.1029/2004WR003800.

Wooding, R. A. (1997), A hydraulic model for the catchment-stream problem. 1. Kinematic-wave theory, *J. Hydrol.*, *191*(1–4), 371–371.

Xu, N., and J. E. Saiers (2010), Temperature and hydrologic controls on dissolved organic matter mobilization and transport within a forest topsoil, *Environ. Sci. Technol.*, *44*(14), 5423–5429, doi:10.1021/es1002296.

Yano, Y., K. Lajtha, P. Sollins, and B. A. Caldwell (2004), Chemical and seasonal controls on the dynamics of dissolved organic matter in a coniferous old-growth stand in the Pacific Northwest, USA, *Biogeochemistry*, *71*(2), 197–223, doi:10.1007/s10533-004-8130-8.

Yurova, A., A. Sirin, I. Buffam, K. Bishop, and H. Laudon (2008), Modeling the dissolved organic carbon output from a boreal mire using the convection-dispersion equation: Importance of representing sorption, *Water Resour. Res.*, *44*, W07411, doi:10.1029/2007WR006523.

Zehe, E., and M. Sivapalan (2009), Threshold behaviour in hydrological systems as (human) geo-ecosystems: Manifestations, controls, implications, *Hydrol. Earth Syst. Sci.*, *13*(7), 1273–1297.

P. A. Raymond, J. E. Saiers, and N. Xu, School of Forestry and Environmental Studies, Yale University, 195 Prospect St., New Haven, CT 06520, USA. (james.saiers@yale.edu)

H. F. Wilson, Brandon Research Center, Agriculture and Agri-Food Canada, 2701 Grand Valley Rd., Box 1000A, Rt. 3, Brandon, Manitoba R7A 5Y3, Canada.